Table 1 Single-nucleotide polymorphism (SNP), genotyping methods and possible functional role

SNP nucleotide/amino acid change	**Database ID**	**Genotyping method**	**Chromosome/exon or intron**	**MAF (%) in different populations** (NCBI dbSNP)	**SNP effects, minor allele versus wild-type** (reference)
ATM G5557A Asp1853Asn	rs1801516	PCR/RFLP[a] (AflII) GG (187, 30) GA (217, 187, 30) AA (217)	11/exon 39	European: 7–22 Asian: 0–2 Global: 5	Alters an exonic splicing enhancer, modulates correct splicing of exon 39 (Thorstenson *et al.* 2003) Decreases *ATM* expression level and capacity of DNA damage recognition (Heikkinen *et al.* 2005)
ATM IVS22−77 T>C T60136C	rs664677	PCR/RFLP (RsaI) TT (299) TC (299, 265, 34) CC (265, 34)	11/intron 22	European: 34–50 Asian: 44–70 Global: 35–36	No reports
ATM IVS48+238 C>G C113450G	rs609429	PCR/RFLP (KpnI) CC (172, 35) CG (207, 172, 35) GG (207)	11/intron 48	European: 60 Asian: 37 Global: 53	Generates a week additional donor splice site and decreases gene expression (Angele *et al.* 2003)
XRCC1 G25211A Arg280His	rs25489	PCR/RFLP (RsaI) GG (155, 123) GA (278, 155, 123) AA (278)	19/exon 9	European: 3–10 Asian: 0 Global: 7	Compromises DNA repair (reviewed by Hu *et al.* 2005)
XRCC1 G25897A Arg399Gln	rs25487	PCR/RFLP (MspI) GG (327, 107) GA (434, 327, 107) AA (434)	19/exon 10	European: 30–46 Asian: 27 Global: 23–26	Affects IR-induced mitotic delay and hypersensitivity to IR (Hu *et al.* 2002) Compromises single-strand DNA breaks repair (controversially) (reviewed by Taylor *et al.* 2002)
TP53 G640C Arg72Pro	rs1042522	TaqMan	17/exon 4	European: 23–27 Asian: 40–51 Global: 35	Lower efficiency in apoptosis induction; higher level of G1 arrest (Pim & Banks 2004)
XRCC3 C18067T Thr241Met	rs861539	TaqMan	14/exon 7	European: 41–45 Asian: 6–14 Global: 22	Decreased DNA repair capacity (reviewed by Han *et al.* 2006)
MTF1 T2193A	rs11488567	Melting curve T_m-shift	1/intron 1	Unknown	No reports
MTF1 G20433A	rs3912368	Melting curve T_m-shift	1/intron 5	European: 25–37 Asian: 21	No reports

[a]Restriction enzymes, genotypes and corresponding restriction fragments sizes (bp) are indicated for the SNPs analyzed by PCR/RFLP.

Table 2 Primers and probes for genotyping

SNP	Primer/probe sequences (5′–3′)[a]	Primer/probe concentration (μM)	Annealing temperature (°C)
ATM G5557A	F: CCATACTTGATTCATGATATTTTACcttAA	0.2	57
	R: TTCCATCTTAAATCCATCTTTCTC	0.2	
ATM IVS22−77 T>C	F: AGTTTAGCACAGAAAGACATATTGGAAGTAACgTA	0.2	57
	R: CGGGAAAAGAACTGTGGTTAAATATGAAA	0.2	
ATM IVS48+238 C>G	F: CTCAATTTCCTGGTTATAAAATGAGAAGgTAC	0.2	57
	R: TTAACTACTTGTCAGGGACTATCTTAAGGAC	0.2	
XRCC1 G25211A	F: GTCTGAGGGAGGAGGGTCTG	0.2	59
	R: TTCTGGAAGCCACTCAGCAC	0.2	
XRCC1 G25897A	F: CCACCAGCTGTGCCTTTG	0.2	55
	R: CCGGGACTCACTTTGAATGA	0.2	
TP53 G640C	F: CGTCCCAAGCAATGGATGATT	0.8	61
	R: CCGGTGTAGGAGCTGCTGG	0.8	
	w/t allele probe (FAM): CTCCCCGCGTGGCCCC	0.4	
	Variant allele probe (VIC): CTCCCCCCGTGGCCCC	0.4	
XRCC3 C18067T	F: AGGGCCAGGCATCTGCA	0.8	61
	R: CTTCCGCATCCTGGCTAA	0.8	
	w/t allele probe (FAM): TCACGCAGCGTGGCCCCCAG	0.5	
	Variant allele probe (VIC): TCACGCAGCATGGCCCCCAG	0.5	
MTF1 T2193A	F1: GCGGGCAGGGCGGCTTAACTTTAAAACCATCAAGTCATTTTTAgA	0.2	58
	F2: GCGGGCTTAACTTTAAAACCATCAAGTCATTTTTAAT	0.2	
	R: ACGCCCAGTCGGCATTGCT	0.2	
MTF1 G20433A	F1: GCGGGCAGGGCGGCCTAATTATGCTCACCTGAATATATACAGGG	0.075	63
	F2: GCGGGCCTAATTATGCTCACCTGAATATATACAGGA	0.2	
	R: GAGACCTGTAGAGCTAGGTGGATATACAGAGATAT	0.2	

[a]The bases shown in lowercase are mismatches introduced to generate restriction endonuclease sites (PCR/RFLP) or to optimize allelic specificity (T_m-shift). The underlined 5′ portions of primer sequences correspond to GC tails in the T_m-shift method.

Raw genotyping outputs were interpreted by at least two independent investigators. Missing results due to genotyping procedure failures accounted for <1% for any SNP tested.

Statistical analysis

Genotype frequencies in each group were determined by univariate analysis and evaluated for departure from Hardy-Weinberg equilibrium by the χ^2 test. SNP associations with PTC were assessed by multivariate logistic regression analysis for codominant, multiplicative, dominant, and recessive models to avoid assumptions regarding the mode of inheritance (see notes below Table 4). All analyses were adjusted for gender (male or female, nominal), age (years, continuous), and IR-exposure (yes or no, nominal). Besides all the parameters above, the full model included disease status (yes or no, nominal) and, depending on the mode of inheritance, genotype for each SNP (nominal variable in the codominant, dominant, and recessive models and ordinal in the multiplicative model).

Power calculations were done with the PS software (http://biostat.mc.vanderbilt.edu/twiki/bin/view/Main/PowerSampleSize). With given sample size, the study had a power of 54–99% to detect an OR of 2.0 at the significance level of 5% with MAF ranging 4–45%.

Interaction between SNPs, cancer and radiation exposure were hypothesized *a priori* and evaluated by multivariate analysis with corresponding adjustments. Separate calculations of OR were done in irradiated and non-exposed case–control groups when *P* value for an interaction term did not exceed 0.05.

Statistical analysis was done using SPSS for Windows version 17.0 (SPSS, Inc., Chicago, IL, USA).

Results

The distribution of genotypes and MAF for each SNP in the four study groups is shown in Table 3. The observed distributions in the control groups were not statistically different from those expected from Hardy-Weinberg equilibrium for all SNP except for *ATM* G5557A and *ATM* IVS22-77 T>C in the non-exposed controls. Since such deviation might point at possible genotyping error (Hosking *et al.* 2004), we reanalyzed 96 non-exposed controls for these SNPs by direct sequencing. There were no inconsistencies between PCR/RFLP and sequencing results (data not shown) ruling out technical flaw. Furthermore, allelic frequencies determined in our study are in a good agreement

Table 3 Distribution of genotypes and minor allele frequencies by study groups

SNP, genotype	IR-induced PTC *n* (%)	IR-exposed controls *n* (%)	Sporadic PTC *n* (%)	Non-exposed controls *n* (%)
ATM G5557A	*n*=122	*n*=198	*n*=132	*n*=398
GG	95 (77.9)	138 (69.7)	105 (79.5)	293 (73.6)
GA	25 (20.5)	53 (26.8)	24 (18.2)	90 (22.6)
AA	2 (1.6)	7 (3.5)	3 (2.3)	15 (3.8)
P	0.24		0.36	
A, %	11.9	16.9	11.4	15.1
ATM IVS22−77 T>C	*n*=123	*n*=195	*n*=132	*n*=398
TT	35 (28.4)	62 (31.8)	45 (34.1)	135 (33.9)
TC	76 (61.8)	102 (52.3)	61 (46.2)	216 (54.3)
CC	12 (9.8)	31 (15.9)	26 (19.7)	47 (11.8)
P	0.17		0.06	
C, %	40.6	42.0	42.8	38.9
ATM IVS48+238 C>G	*n*=122	*n*=196	*n*=132	*n*=398
CC	37 (30.3)	68 (34.7)	41 (31.1)	131 (32.9)
CG	69 (56.6)	97 (49.5)	61 (46.2)	201 (50.5)
GG	16 (13.1)	31 (15.8)	30 (22.7)	66 (16.6)
P	0.47		0.28	
G, %	41.4	40.3	45.8	41.8
XRCC1 Arg280His[a]	*n*=123	*n*=195	*n*=132	*n*=398
GG	113 (91.9)	176 (90.3)	117 (88.6)	366 (92.0)
GA	10 (8.1)	19 (9.7)	15 (11.4)	32 (8.0)
P	0.63		0.24	
A, %	4.1	4.9	5.7	4.0
XRCC1 Arg399Gln	*n*=123	*n*=197	*n*=132	*n*=398
GG	55 (44.7)	75 (38.1)	65 (49.2)	158 (39.7)
GA	50 (40.7)	100 (50.7)	53 (40.2)	193 (48.5)
AA	18 (14.6)	22 (11.2)	14 (10.6)	47 (11.8)
P	0.20		0.15	
A, %	35.1	36.5	30.7	36.1
TP53 Arg72Pro	*n*=122	*n*=197	*n*=129	*n*=395
GG	53 (43.4)	115 (58.4)	69 (53.5)	196 (49.6)
GC	57 (46.7)	73 (37.0)	49 (38.0)	161 (40.8)
CC	12 (9.9)	9 (4.6)	11 (8.5)	38 (9.6)
P	0.02		0.74	
C, %	33.2	23.1	27.5	30.0
XRCC3 Thr241Met	*n*=120	*n*=198	*n*=132	*n*=398
CC	53 (44.2)	82 (41.4)	55 (41.7)	161 (40.5)
CT	51 (42.5)	89 (45.0)	65 (49.2)	192 (48.2)
TT	16 (13.3)	27 (13.6)	12 (9.1)	45 (11.3)
P	0.89		0.78	
T, %	34.6	36.1	33.7	35.4
MTF1 T2193A	*n*=122	*n*=198	*n*=131	*n*=397
TT	45 (36.9)	82 (41.4)	44 (33.6)	133 (33.5)
TA	64 (52.5)	91 (46.0)	67 (51.1)	188 (47.4)
AA	13 (10.6)	25 (12.1)	20 (15.3)	76 (19.1)
P	0.52		0.57	
A, %	36.8	35.6	40.8	42.8
MTF1 G20433A	*n*=123	*n*=198	*n*=132	*n*=398
GG	62 (50.4)	100 (50.5)	66 (50.0)	192 (48.2)
GA	53 (43.1)	88 (44.4)	56 (42.4)	151 (38.0)
AA	8 (6.5)	10 (5.1)	10 (7.6)	55 (13.8)
P	0.85		0.16	
A, %	28.0	27.3	28.8	32.8

NOTE. Total numbers of samples in each group vary slightly due to genotyping procedures failures.
[a]There was no homozygous (A/A) variant of XRCC1 Arg280His among all samples tested.

with those specified for Caucasians in the dbSNP (build 129, April 2008, Table 1) thus attesting to the appropriate data quality.

As seen from Table 4, an association between *ATM* G5557A and PTC, regardless of radiation exposure, was found. The presence of the A allele significantly decreased PTC risk compared with wild-type G allele in the multiplicative model of inheritance (OR=0.69, 95% CI 0.45–0.86, $P=0.03$), which is useful for risk comparison between the groups based on the analysis of allelic frequencies in them.

Main effect on PTC risk appeared also significant for the *XRCC1* gene Arg399Gln polymorphism. The presence of the minor 399Gln allele decreased PTC risk compared with the Arg/Arg genotype (OR=0.66, 95% CI 0.57–0.88, $P=0.02$ and OR=0.70, 95% CI 0.59–0.93, $P=0.03$, in the co-dominant and dominant models respectively).

Analysis of combined *ATM* G5557A and *XRCC1* Arg399Gln genotypes demonstrated that increasing number of minor alleles (i.e. *ATM* 5557A and *XRCC1* 399Gln) significantly decreased PTC risk in corresponding individuals in comparison with those who do not carry minor alleles (Fig. 1).

No other SNP in any gene showed a significant main effect on PTC.

For *ATM* IVS22-77 T>C and *TP53* Arg72Pro, evidence for interaction between radiation exposure and PTC was found (P for interaction 0.04 and 0.01 respectively). As shown in Table 5, the analyses performed in IR-exposed and non-irradiated patients compared respectively, with irradiated and non-exposed controls revealed a significantly increased risk of sporadic PTC for the *ATM* IVS22-77 homozygous CC genotype carriers compared with the TC+TT genotypes (the recessive model of inheritance, OR=1.84, 95% CI 1.10–3.24, $P=0.03$), whereas in the irradiated group an insignificant inverse effect of these genotypes was observed (OR=0.59, 95% CI 0.28–1.27, $P=0.17$). For *TP53* codon 72 polymorphism, in all but the recessive models the increased risk of IR-induced PTC as compared with IR-exposed controls was observed. The highest risk of radiogenic PTC was in the co-dominant model (OR=2.33, 95% CI 1.15–7.21, $P=0.03$). A significant risk was also found in the multiplicative model of inheritance (OR=1.70, 95% CI 1.17–2.46, $P=0.006$). In addition, comparison between IR-exposed and non-exposed controls did not reveal statistically significant difference in adjusted distributions of these polymorphisms. In healthy subjects, the strongest association for the *ATM* IVS22-77 T>C was in the recessive model (OR=1.38, 95% CI 0.84–2.26, $P=0.21$) and in the multiplicative model for *TP53* Arg72Pro (OR=0.70, 95% CI 0.52–1.19, $P=0.11$) further emphasizing possible role of these SNPs in PTC of different etiology.

Considering multiple pathways for repairing diverse DNA damages induced by endogenous and exogenous carcinogens, genetic variants in different repair pathways may probably have a joint effect on cancer risk. In attempt to search for the stronger associations between PTC and studied SNPs, we performed the analyses of genotype combinations for the *ATM* and *TP53* polymorphisms as these genes are functionally related and three out of four SNPs included in our study showed effects on PTC. Among the possible *ATM/TP53* combinations (rs1801516/rs664677/rs609429/rs1042522) tested, two demonstrated significant differences in the subsets of both groups of PTCs (Fig. 2). Particularly, the combined *ATM/TP53* GG/TC/CG/GC genotype was strongly associated with the IR-induced PTC (OR=2.10, 95% CI 1.17–3.78, $P=0.015$). Another *ATM/TP53* combination, GG/CC/GG/GG, demonstrated a significantly increased risk for sporadic PTC (OR=3.32, 95% CI 1.57–6.99, $P=0.002$).

Discussion

Our study addressed possible associations between SNPs in the genes involved in DNA damage response and the risk of PTC of different etiology. The results demonstrated that the presence of the variant 5557A allele in exon 39 of *ATM* and *XRCC1* 399Gln allele, particularly in the heterozygous state, significantly associated with the decreased risk of PTC. The *ATM* IVS22-77 CC genotype in the non-exposed group and the *TP53* 72Pro allele in the radiation-related one associated with the increased risk of PTC. Moreover, two particular *ATM/TP53* combined genotypes were found with higher frequencies in the IR-induced or sporadic PTC when compared with the controls. Altogether, these data indicate that SNPs in the studied genes may likely modify PTC risk.

A significant association between the *ATM* G5557A and bilateral breast cancer in Caucasian patients has been shown before (Heikkinen *et al.* 2005). Also, this SNP has been reported as a possible modulator of clinical radiosensitivity in cancer. The *ATM* 5557A allele was associated with severe adverse effects of radiation therapy in prostate (Hall *et al.* 1998) and breast cancer patients (Angele *et al.* 2003). Later, an enhanced radiosensitivity of human fibroblasts in the presence of the *ATM* 5557A allele was demonstrated in an experimental work (Alsbeih *et al.* 2007). In contrast

Table 4 OR (95% CI) for papillary thyroid carcinoma (PTC) by gene polymorphism according to different models of inheritance (adjusted for age, gender and radiation exposure). $P < 0.05$ in bold

SNP	Genotype	OR (95% CI)	P
ATM G5557A	*GG*	1.00[a]	
	GA	0.75 (0.49–1.15)	0.31
	AA	0.61 (0.21–1.77)	0.45
	Risk per *A* allele[b]	0.69 (0.45–0.86)	**0.03**
	GA+*AA* versus *GG*[c]	0.73 (0.48–1.10)	0.13
	AA versus *GA*+*GG*[d]	0.65 (0.23–1.87)	0.41
ATM IVS22−77 T>C	*TT*	1.00	
	TC	1.03 (0.70–1.50)	0.74
	CC	1.19 (0.70–2.04)	0.47
	Risk per *C* allele	1.08 (0.83–1.40)	0.57
	TC+*CC* versus *TT*	1.06 (0.74–1.53)	0.75
	CC versus *TC*+*TT*	1.17 (0.72–1.90)	0.52
ATM IVS48+238 C>G	*CC*	1.00	
	CG	1.10 (0.75–1.62)	0.55
	GG	1.14 (0.69–1.89)	0.84
	Risk per *G* allele	1.07 (0.84–1.37)	0.57
	CG+*GG* versus *CC*	1.11 (0.77–1.60)	0.57
	GG versus *CG*+*CC*	1.08 (0.69–1.69)	0.74
XRCC1 Arg280His[e]	*GG*	1.00	
	GA	1.12 (0.62–2.01)	0.71
	Risk per *A* allele	1.15 (0.70–1.87)	0.61
XRCC1 Arg399Gln	*GG*	1.00	
	GA	0.66 (0.57–0.88)	**0.02**
	AA	0.88 (0.50–1.57)	0.56
	Risk per *A* allele	0.90 (0.69–1.17)	0.41
	GA+*AA* versus *GG*	0.70 (0.59–0.93)	**0.03**
	AA versus *GA*+*GG*	0.98 (0.57–1.69)	0.94
TP53 Arg72Pro	*GG*	1.00	
	GC	1.02 (0.70–1.47)	0.89
	CC	1.16 (0.63–2.14)	0.38
	Risk per *C* allele	1.05 (0.81–1.38)	0.70
	GC+*CC* versus *GG*	1.04 (0.74–1.48)	0.82
	CC versus *GC*+*GG*	1.15 (0.64–2.08)	0.64
XRCC3 Thr241Met	*CC*	1.00	
	CT	0.99 (0.69–1.44)	0.99
	TT	0.96 (0.54–1.70)	0.92
	Risk per *T* allele	0.99 (0.76–1.28)	0.92
	CT+*TT* versus *CC*	0.99 (0.70–1.41)	0.97
	TT versus *CT*+*CC*	0.96 (0.56–1.64)	0.88
MTF1 T2193A	*TT*	1.00	
	TA	1.07 (0.73–1.56)	0.61
	AA	0.83 (0.49–1.41)	0.46
	Risk per *A* allele	0.94 (0.73–1.21)	0.63
	TA+*AA* versus *TT*	1.00 (0.70–1.44)	0.99
	AA versus *TA*+*TT*	0.80 (0.49–1.29)	0.35
MTF1 G20433A	*GG*	1.00	
	GA	1.14 (0.79–1.63)	0.43
	AA	0.76 (0.40–1.43)	0.21
	Risk per *A* allele	0.97 (0.74–1.25)	0.80
	GA+*AA* versus *GG*	1.05 (0.76–1.49)	0.76
	AA versus *GA*+*GG*	0.71 (0.39–1.32)	0.27

[a]Codominant model of inheritance (wild-type homozygous genotype serves as the reference).
[b]Multiplicative model of inheritance (uses allele frequencies).
[c]Dominant inheritance model (combined heterozygous and homozygous for the minor allele versus wild-type homozygous).
[d]Recessive inheritance model (minor allele homozygous versus combined heterozygous and homozygous for the wild-type allele).
[e]The dominant and recessive models are not shown for *XRCC1* Arg280His because of the absence of homozygous (A/A) genotype among 848 samples tested.

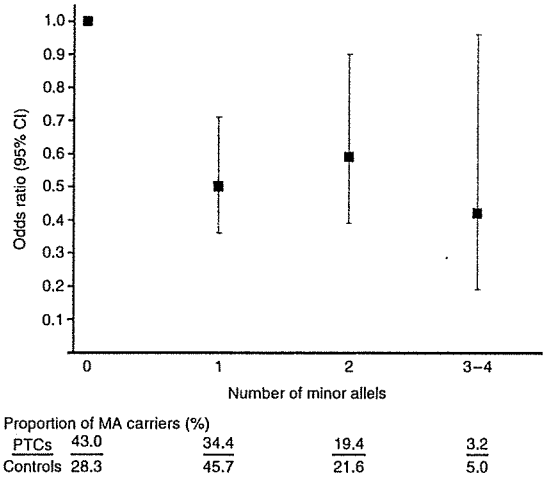

Figure 1 Effect of increasing number of minor alleles (MA) for *ATM* G5557A and *XRCC1* Arg399Gln (minor alleles, *ATM* 5557A, and *XRCC1* 399Gln) on PTC risk. The combined genotype with 0 MA was used as a reference. *P* values for genotypes with different MA number: $P_{1MA}<0.0001$; $P_{2MA}<0.01$; $P_{3-4MA}<0.05$. Carriers of three and four minor alleles were combined because of the exceedingly low number of 4 MA carriers in both PTC and control groups.

to these reports, Edvardsen *et al.* (2007) revealed an increasing rate of side effects of radiotherapy with decreasing frequency of this variant allele. Our data are rather in agreement with the latter report and favor the protective role of the *ATM* 5557A allele in PTC development.

The intronic *ATM* polymorphisms IVS22–77 T>C and IVS48+238 C>G in the homozygous state have been associated with increased breast cancer risk and in the heterozygous state with clinical radioprotection (Angele *et al.* 2003). These findings were confirmed in the *in vitro* experiments using lymphoblastoid cell lines established from corresponding patients. Our investigation demonstrated the association between the IVS22–77 CC genotype and increased risk of sporadic PTC in adult patients. By contrast, in the IR-induced PTC group, there was an inverse non-insignificant correlation for this genotype. At the same time, in the IR-induced PTCs, the number of patients heterozygous for IVS22–77 was somewhat, but insignificantly, higher as compared with sporadic PTCs (Table 3). The results for the IVS48+238 C>G tended to parallel those for the IVS22–77 T>C remaining below the threshold of significance. At present, the mechanistic and functional basis for the intronic *ATM* SNPs implications in cancer revealed in the previous studies and in ours as well is not fully understood. In a broader sense, however, they may be indicative of a role for the *ATM* gene (or its product) in the development of PTC.

As reviewed by Hu *et al.* (2005), the results of the *XRCC1* gene Arg399Glu investigations vary in different cancers for populations with different ethnicities. In relation to cancer and radiation, the 399Gln allele in combination with 280His was associated with breast cancer risk, and in pair with 194Trp with clinical radiosensitivity in Caucasian women with breast cancer. Also, the 399Gln allele was found to decrease

Table 5 OR (95% CI) for papillary thyroid carcinoma (PTC) of different etiology by *ATM* and *TP53* polymorphisms (adjusted for gender and age). *P* <0.05 in bold

		IR-induced PTC versus IR-exposed controls		Sporadic PTC versus non-exposed controls	
SNP	**Genotype**	**OR (95% CI)**	***P***	**OR (95% CI)**	***P***
ATM IVS22−77 T>C	*TT*	1.00[a]		1.00	
	TC	1.38 (0.80–2.39)	0.19	0.82 (0.51–1.32)	0.50
	CC	0.73 (0.31–1.70)	0.44	1.63 (0.87–3.08)	0.09
	Risk per *C* allele[b]	0.97 (0.66–1.41)	0.86	1.18 (0.86–1.62)	0.32
	TC+*CC* versus *TT*[c]	1.23 (0.72–2.10)	0.44	0.97 (0.62–1.52)	0.88
	CC versus *TC*+*TT*[d]	0.59 (0.28–1.27)	0.17	1.84 (1.10–3.24)	**0.03**
TP53 Arg72Pro	*GG*	1.00		1.00	
	GC	1.68 (1.11–2.75)	**0.03**	0.84 (0.53–1.33)	0.52
	CC	2.33 (1.15–7.21)	**0.03**	0.84 (0.39–1.79)	0.73
	Risk per *C* allele	1.70 (1.17–2.46)	**0.006**	0.89 (0.64–1.23)	0.47
	GC+*CC* versus *GG*	1.80 (1.06–2.36)	**0.01**	0.84 (0.54–1.29)	0.43
	CC versus *GC*+*GG*	2.06 (0.79–5.41)	0.14	0.90 (0.44–1.88)	0.79

[a]Codominant model of inheritance (wild-type homozygous genotype serves as the reference).
[b]Multiplicative model of inheritance (uses allele frequencies).
[c]Dominant inheritance model (combined heterozygous and homozygous for the minor allele versus wild-type homozygous).
[d]Recessive inheritance model (minor allele homozygous versus combined heterozygous and homozygous for the wild-type allele).

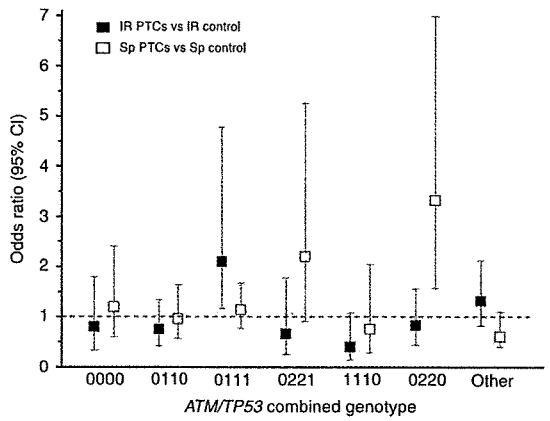

Proportion of carriers, (%)	IR	Sp	IR	Sp	IR	Sp	IR	Sp	IR	Sp	IR	Sp	IR	Sp
PTCs	7.3	9.0	17.8	17.4	*24.8*	15.5	5.0	7.1	4.0	3.8	3.3	*11.8*	38.0	35.6
Controls	9.3	8.0	21.7	17.5	*13.5*	14.2	7.1	3.3	10.0	5.2	6.2	*3.8*	32.0	48.0

Figure 2 The combined *ATM/TP53* genotypes and risk of PTC of different etiology. The combined genotypes were analyzed separately in the IR-exposed and sporadic PTCs versus corresponding control. Six combinations of 3 *ATM* and 1 *TP53* SNPs (rs1801516/rs664677/rs609429/rs1042522) whose frequencies were higher than 5% at least in two of four subgroups are shown. In the numerical codes for any SNP, 0 – the genotype with no MA (i.e. homozygous wild-type); 1 – 1 MA presents (heterozygous genotype); 2 – 2 MA present (homozygous variant genotype); first three numbers correspond to 3 *ATM* SNPs and the last one to *TP53* polymorphism. In the figure, the *GG/TT/CC/GG* genotype is represented by the '0000' numerical code as it does not contain minor alleles; the *GG/TC/CG/GG* corresponds to 0110, *GG/TC/CG/GC* to 0111; *GG/CC/GG/GC* to 0221; *GA/TC/CG/GG* to 1110, and *GG/CC/GG/GG* to 0220. All combinations with frequencies <5% in three or more subgroups are pooled and indicated as 'other'.

the risk of bladder cancer and squamous cell carcinoma of the head and neck.

Interestingly, not only variant but also wild-type allele (i.e. *XRCC1* 399Arg) demonstrated possible role in cancer. High-dose radiation to the chest was more strongly associated with breast cancer among white American women with *XRCC1* Arg399Arg genotype (Duell *et al.* 2001). Looking for potential biological explanations for these findings, the authors found a higher prevalence of *TP53* deletions in the Arg399Arg cases exposed to occupational radiation compared with exposed patients with the Gln399Gln genotypes or unexposed cases of either genotype. Figueiredo *et al.* (2004) observed an increased risk of disease among wild-type homozygous (Arg/Arg) and heterozygous Canadian Caucasian women with a family history of breast cancer compared with the individuals without such.

The described above data may be explained, at least in part, by the results of functional study of this polymorphism in which an equal ability for both alleles to suffice single strand break repair by *XRCC1* has been found (Taylor *et al.* 2002). The results of our study, taken together with those reported previously, suggest that *XRCC1* polymorphism in particular the Arg399Gln genotype may influence PTC risk, perhaps by modifying the effects of environmental exposure and/or through interaction with other genetic factors.

The *TP53* Arg72Pro polymorphism affects the biological activity of p53. The Arg72 form is more efficient at inducing apoptosis while the Pro72 appears to induce a higher level of G1 arrest (Pim & Banks 2004). Based on these findings, a number of studies have attempted to assess a correlation between *TP53* codon 72 polymorphism and risk of certain types of cancer, however, with inconsistent results, as reviewed by Pietsch *et al.* (2006). This inconsistency may possibly be explained in part by the coexistence of the codon 72 polymorphism and gain of function mutations in *TP53* in some tumors (Pietsch *et al.* 2006, Soussi & Wiman 2007).

Several groups have investigated the TP53 Arg72-Pro polymorphism in PTC. Boltze *et al.* (2002) found a small number of heterozygotes and no Pro/Pro genotype in differentiated thyroid carcinomas from Germany. By contrast, in ethnically heterogeneous Brazilian population, the Pro/Pro genotype was associated with the higher risk of differentiated thyroid cancer (Granja *et al.* 2004). The study of codon 72 polymorphism in thyroid tumors from Russian and Ukrainian patients demonstrated a significantly lower frequency of wild-type homozygotes (i.e. Arg/Arg) among adults with IR-induced PTC when compared with sporadic PTC cases and general population (Rogounovitch *et al.* 2006). Data obtained in the present work, using an independent set of samples, confirm these findings suggesting the modifying role (or as of a marker) of the TP53 Arg72Pro polymorphism in PTC developed after exposure to IR which is further supported by the absence of significant difference in genotype distributions among our two control groups.

As shown in a genetic study, frequencies of the *C* allele (encoding 72Pro) do not generally differ in populations of Belarus and Russia (Khrunin *et al.* 2005). However, East Slavs do not form a single genetic cluster on multidimensional analysis. The 72Pro allele frequency in Belarus is about 0.3; in the two different subpopulations from the Central and Northern regions of the European part of Russia it is 0.24 and 0.32 respectively. The study of healthy population from Poland (bordering with Belarus, linguistically and culturally similar), reported the frequency of 0.28 for the 72Pro allele (Siddique *et al.* 2005). The 72Pro frequency reported by

Rogounovitch *et al.* (2006) in Russian healthy controls is also 0.28. Thus, the effect of population admixtures in the controls in our investigation could not be completely ruled out. Yet on the other hand, the ratio of Belarusian and Russian subjects in the IR-exposed PTCs and controls was similar (2.24 and 2.30 respectively) suggestive of an unbiased estimate and being an argument in support of *TP53* Arg72Pro polymorphism association with radiation-related PTC.

While many studies established the effect of individual SNPs on cancer, the role of SNP combinations has been less addressed. Several *ATM* and *TP53* haplotypes were associated with clinical radiosensitivity in breast cancer (Angele *et al.* 2003) and brain tumor risk (Malmer *et al.* 2007). Recently, the interactions of SNPs located on different chromosomes were investigated in various malignancies (Yen *et al.* 2008, Yoon *et al.* 2008). One experimental study, in which *ATM* Asp1853Asn, *TP53* Arg72Pro, *XRCC1* Arg399Gln, and *XRCC3* Thr241Met were genotyped, demonstrated that the increasing number of risk alleles enhanced radiosensitivity of human fibroblast cell lines and, potentially, susceptibility to radiation-induced cancers (Alsbeih *et al.* 2007). So far no studies have investigated the joint effect of gene polymorphisms on thyroid cancer. Our observations demonstrated that frequencies of particular combined *ATM/TP53* genotypes were higher in patients with radiogenic or sporadic PTC compared with corresponding control populations.

To some extent these results support the idea that genetic factors may possibly modify predisposition to thyroid cancer. A recent study by Detours *et al.* (2007) reported difference in the expression levels of some genes between Chernobyl PTCs from Ukraine and French sporadic PTCs. Although the mentioned work and the present one are different in molecular approaches, the results of both are suggestive of a possible genetic 'susceptibility signature' that may contribute to the individual predisposition to IR and other carcinogens' effects. These findings are in favor of a 'susceptibility model' that may partly explain why only a minority of the large population exposed to the IR after the Chernobyl disaster developed thyroid cancer (Yamashita & Saenko 2006, Detours *et al.* 2007, 2008).

It is necessary to note that even though nine SNPs were analyzed in our study, no correction for multiple comparisons was applied because of study design and techniques employed. The associations were tested in a one-at-a-time fashion in a limited sample size in the difficult to access groups. The need for correction in such circumstances is still debated (Rothman & Greenland 1998). Furthermore, since data obtained in this work may be referred to as an initial screening result, non-adjusted presentation enables their inclusion in future meta-analysis. Effects of candidate SNPs that we report need validation in other studies.

In conclusion, the results presented here show that SNPs in *ATM* exon 39 and *XRCC1* exon 10 may be the markers of a decreased PTC risk in adults, whereas the *ATM* IVS22-77 and *TP53* codon 72 SNPs genes may associate with the risk of PTC development in non-irradiated and irradiated individuals. To the best of our knowledge, presented here is the first study of this kind reporting the results of genotyping of candidate DNA damage response genes in irradiated and non-irradiated PTC patients and in corresponding healthy populations. Our data support the paradigm of genetic modifiers of radiation-associated carcinogenesis and perhaps may contribute to genetic determination of PTC-prone subjects. We believe such identification will allow future personalized cancer risk prediction which is of a significant importance in view of the growing thyroid cancer incidence and also because of the relevance to occupational and radiation emergency medicine issues.

Declaration of interest

The authors declare no potential conflict of interest.

Funding

This work was supported in part by Grant-in-Aid for Scientific Research 19256003, 19510058, and 19790651 from Japan Society for the Promotion of Science.

References

Alsbeih G, El-Sebaie M, Al-Harbi N, Al-Buhairi M, Al-Hadyan K & Al-Rajhi N 2007 Radiosensitivity of human fibroblasts is associated with amino acid substitution variants in susceptible genes and correlates with the number of risk alleles. *International Journal of Radiation Oncology, Biology, Physics* **68** 229–235.

Angele S, Romestaing P, Moullan N, Vuillaume M, Chapot B, Friesen M, Jongmans W, Cox DG, Pisani P, Gerard JP *et al.* 2003 ATM haplotypes and cellular response to DNA damage: association with breast cancer risk and clinical radiosensitivity. *Cancer Research* **63** 8717–8725.

Bennett B, Repacholi M & Carr Z 2006 *Health Effects of the Chernobyl Accident and Special Health Care Programmes*. Geneva: WHO Press.

Boltze C, Roessner A, Landt O, Szibor R, Peters B & Schneider-Stock R 2002 Homozygous proline at codon 72

of p53 as a potential risk factor favoring the development of undifferentiated thyroid carcinoma. *International Journal of Oncology* **21** 1151–1154.

Bouville A, Likhtarev IA, Kovgan L, Minenko VF, Shinkarev SM & Drozdovitch V 2007 Radiation dosimetry for highly contaminated Belarusian, Russian and Ukranian populations, and for less contaminated populations in Europe. *Health Physics* **93** 487–501.

Cardis E, Kesminiene A, Ivanov V, Malakhova I, Shibata Y, Khrouch V, Drozdovitch V, Maceika E, Zvonova I, Vlassov O *et al.* 2005 Risk of thyroid cancer after exposure to ^{131}I in childhood. *Journal of the National Cancer Institute* **97** 724–732.

Davies L & Welch HG 2006 Increasing incidence of thyroid cancer in the United States, 1973–2002. *Journal of the American Medical Association* **295** 2164–2167.

Davis S, Stepanenko V, Rivkind N, Kopecky KJ, Voilleque P, Shakhtarin V, Parshkov E, Kulikov S, Lushnikov E, Abrosimov A *et al.* 2004 Risk of thyroid cancer in the Bryansk oblast of the Russian Federation after the Chernobyl Power Station accident. *Radiation Research* **162** 241–248.

Detours V, Delys L, Libert F, Weiss Solis D, Bogdanova T, Dumont JE, Franc B, Thomas G & Maenhaut C 2007 Genome-wide gene expression profiling suggests distinct radiation susceptibility in sporadic and post-Chernobyl papillary thyroid cancers. *British Journal of Cancer* **97** 818–825.

Detours V, Versteyhe S, Dumont JE & Maenhaut C 2008 Gene expression profiles of post-Chernobyl thyroid cancers. *Current Opinion in Endocrinology, Diabetes, and Obesity* **15** 440–445.

Duell EJ, Millikan RC, Pittman GS, Winkel S, Lunn RM, Tse CK, Eaton A, Mohrenweiser HW, Newman B & Bell DA 2001 Polymorphisms in the DNA repair gene XRCC1 and breast cancer. *Cancer Epidemiology, Biomarkers & Prevention* **10** 217–222.

Edvardsen H, Tefre T, Jansen L, Vu P, Haffty BG, Fossa SD, Kristensen VN & Borresen-Dale AL 2007 Linkage disequilibrium pattern of the ATM gene in breast cancer patients and controls; association of SNPs and haplotypes to radio-sensitivity and post-lumpectomy local recurrence. *Radiation Oncology* **2** 25.

Figueiredo JC, Knight JA, Briollais L, Andrulis IL & Ozcelik H 2004 Polymorphisms XRCC1-R399Q and XRCC3-T241M and the risk of breast cancer at the Ontario site of the Breast Cancer Family Registry. *Cancer Epidemiology, Biomarkers & Prevention* **13** 583–591.

Granja F, Morari J, Morari EC, Correa LA, Assumpcao LV & Ward LS 2004 Proline homozygosity in codon 72 of p53 is a factor of susceptibility for thyroid cancer. *Cancer Letters* **210** 151–157.

Hall EJ, Schiff PB, Hanks GE, Brenner DJ, Russo J, Chen J, Sawant SG & Pandita TK 1998 A preliminary report: frequency of A-T heterozygotes among prostate cancer patients with severe late responses to radiation therapy. *Cancer Journal from Scientific American* **4** 385–389.

Han S, Zhang HT, Wang Z, Xie Y, Tang R, Mao Y & Li Y 2006 DNA repair gene XRCC3 polymorphisms and cancer risk: a meta-analysis of 48 case–control studies. *European Journal of Human Genetics* **14** 1136–1144.

Heikkinen K, Rapakko K, Karppinen SM, Erkko H, Nieminen P & Winqvist R 2005 Association of common ATM polymorphism with bilateral breast cancer. *International Journal of Cancer* **116** 69–72.

Hillebrandt S, Streffer C, Demidchik EP, Biko J & Reiners C 1997 Polymorphisms in the p53 gene in thyroid tumours and blood samples of children from areas in Belarus. *Mutation Research* **381** 201–207.

Hoeijmakers JH 2001 Genome maintenance mechanisms for preventing cancer. *Nature* **411** 366–374.

Hosking L, Lumsden S, Lewis K, Yeo A, McCarthy L, Bansal A, Riley J, Purvis I & Xu CF 2004 Detection of genotyping errors by Hardy-Weinberg equilibrium testing. *European Journal of Human Genetics* **12** 395–399.

Hu JJ, Smith TR, Miller MS, Lohman K & Case LD 2002 Genetic regulation of ionizing radiation sensitivity and breast cancer risk. *Environmental and Molecular Mutagenesis* **39** 208–215.

Hu Z, Ma H, Chen F, Wei Q & Shen H 2005 XRCC1 polymorphisms and cancer risk: a meta-analysis of 38 case–control studies. *Cancer Epidemiology, Biomarkers & Prevention* **14** 1810–1818.

Jacob P, Bogdanova TI, Buglova E, Chepurniy M, Demidchik Y, Gavrilin Y, Kenigsberg J, Meckbach R, Schotola C, Shinkarev S *et al.* 2006 Thyroid cancer risk in areas of Ukraine and Belarus affected by the Chernobyl accident. *Radiation Research* **165** 1–8.

Khanna KK & Jackson SP 2001 DNA double-strand breaks: signaling, repair and the cancer connection. *Nature Genetics* **27** 247–254.

Khrunin AV, Tarskaia LA, Spitsyn VA, Lylova OI, Bebyakova NA, Mikulich AI & Limborska SA 2005 p53 polymorphisms in Russia and Belarus: correlation of the 2-1-1 haplotype frequency with longitude. *Molecular Genetics and Genomics* **272** 666–672.

Likhtarev I, Bouville A, Kovgan L, Luckyanov N, Voilleque P & Chepurny M 2006 Questionnaire- and measurement-based individual thyroid doses in Ukraine resulting from the Chornobyl nuclear reactor accident. *Radiation Research* **166** 271–286.

Malmer BS, Feychting M, Lonn S, Lindstrom S, Gronberg H, Ahlbom A, Schwartzbaum J, Auvinen A, Collatz-Christensen H, Johansen C *et al.* 2007 Genetic variation in p53 and ATM haplotypes and risk of glioma and meningioma. *Journal of Neuro-oncology* **82** 229–237.

Nikiforov YE, Nikiforova MN, Gnepp DR & Fagin JA 1996 Prevalence of mutations of ras and p53 in benign and malignant thyroid tumors from children exposed to radiation after the Chernobyl nuclear accident. *Oncogene* **13** 687–693.

Nikiforov YE, Rowland JM, Bove KE, Monforte-Munoz H & Fagin JA 1997 Distinct pattern of ret oncogene rearrangements in morphological variants of radiation-induced and sporadic thyroid papillary carcinomas in children. *Cancer Research* **57** 1690–1694.

Pietsch EC, Humbey O & Murphy ME 2006 Polymorphisms in the p53 pathway. *Oncogene* **25** 1602–1611.

Pim D & Banks L 2004 p53 polymorphic variants at codon 72 exert different effects on cell cycle progression. *International Journal of Cancer* **108** 196–199.

Rabes HM, Demidchik EP, Sidorow JD, Lengfelder E, Beimfohr C, Hoelzel D & Klugbauer S 2000 Pattern of radiation-induced RET and NTRK1 rearrangements in 191 post-Chernobyl papillary thyroid carcinomas: biological, phenotypic, and clinical implications. *Clinical Cancer Research* **6** 1093–1103.

Rogounovitch TI, Saenko VA, Ashizawa K, Sedliarou IA, Namba H, Abrosimov AY, Lushnikov EF, Roumiantsev PO, Konova MV, Petoukhova NS *et al.* 2006 TP53 codon 72 polymorphism in radiation-associated human papillary thyroid cancer. *Oncology Reports* **15** 949–956.

Ron E, Lubin JH, Shore RE, Mabuchi K, Modan B, Pottern LM, Schneider AB, Tucker MA & Boice JD Jr 1995 Thyroid cancer after exposure to external radiation: a pooled analysis of seven studies. *Radiation Research* **141** 259–277.

Rothman KJ & Greenland S 1998 *Modern Epidemiology*. 2nd edn. Philadelphia: Lipincott-Raven.

Shiloh Y 2003 ATM and related protein kinases: safeguarding genome integrity. *Nature Reviews. Cancer* **3** 155–168.

Siddique MM, Barlam C, Fiszer-Maliszewska L, Aggarwal A, Tan A, Tan P, Soo KC & Sabapathy K 2005 Evidence for selective expression of the p53 codon 72 polymorphs: implications in cancer development. *Cancer Epidemiology, Biomarkers & Prevention* **14** 2245–2252.

Soussi T & Wiman KG 2007 Shaping genetic alterations in human cancer: the p53 mutation paradigm. *Cancer Cell* **12** 303–312.

Stepanenko VF, Voilleque PG, Gavrilin YuI, Khrouch VT, Shinkarev SM, Orlov MYu, Kondrashov AE, Petin DV, Iaskova EK & Tsyb AF 2004 Estimating individual thyroid doses for a case–control study of childhood thyroid cancer in Bryansk oblast, Russia. *Radiation Protection Dosimetry* **108** 143–160.

Sturgis EM, Zhao C, Zheng R & Wei Q 2005 Radiation response genotype and risk of differentiated thyroid cancer: a case–control analysis. *Laryngoscope* **115** 938–945.

Tamura Y, Maruyama M, Mishima Y, Fujisawa H, Obata M, Kodama Y, Yoshikai Y, Aoyagi Y, Niwa O, Schaffner W *et al.* 2005 Predisposition to mouse thymic lymphomas in response to ionizing radiation depends on variant alleles encoding metal-responsive transcription factor-1 (Mtf-1). *Oncogene* **24** 399–406.

Taylor RM, Thistlethwaite A & Caldecott KW 2002 Central role for the XRCC1 BRCT I domain in mammalian DNA single-strand break repair. *Molecular and Cellular Biology* **22** 2556–2563.

Thorstenson YR, Roxas A, Kroiss R, Jenkins MA, Yu KM, Bachrich T, Muht D, Wayne TL, Chu G, Davis RW *et al.* 2003 Contributions of ATM mutations to familial breast and ovarian cancer. *Cancer Research* **63** 3325–3333.

Wang J, Chuang K, Ahluwalia M, Patel S, Umblas N, Mirel D, Higuchi R & Germer S 2005 High-throughput SNP genotyping by single-tube PCR with T_m-shift primers. *BioTechniques* **39** 885–893.

Williams ED 2006 Chernobyl and thyroid cancer. *Journal of Surgical Oncology* **94** 670–677.

Yamashita S & Saenko V 2006 Mechanisms of disease: molecular genetics of childhood thyroid cancers. *Nature Clinical Practice. Endocrinology & Metabolism* **3** 422–429.

Yang T, Namba H, Hara T, Takamura N, Nagayama Y, Fukata S, Ishikawa N, Kuma K, Ito K & Yamashita S 1997 p53 induced by ionizing radiation mediates DNA end-jointing activity, but not apoptosis of thyroid cells. *Oncogene* **14** 1511–1519.

Yen CY, Liu SY, Chen CH, Tseng HF, Chuang LY, Yang CH, Lin YC, Wen CH, Chiang WF, Ho CH *et al.* 2008 Combinational polymorphisms of four DNA repair genes XRCC1, XRCC2, XRCC3, and XRCC4 and their association with oral cancer in Taiwan. *Journal of Oral Pathology & Medicine* **37** 271–277.

Yoon YJ, Chang HY, Ahn SH, Kim JK, Park YK, Kang DR, Park JY, Myoung SM, Kim do Y, Chon CY *et al.* 2008 MDM2 and p53 polymorphisms are associated with the development of hepatocellular carcinoma in patients with chronic hepatitis B virus infection. *Carcinogenesis* **29** 1192–1196.

The American Journal of Pathology, Vol. 175, No. 4, October 2009

DOI: 10.2353/ajpath.2009.090069

Tumorigenesis and Neoplastic Progression

HMGA1 Is Induced by Wnt/β-Catenin Pathway and Maintains Cell Proliferation in Gastric Cancer

Shin-ichi Akaboshi,*† Sugiko Watanabe,* Yuko Hino,* Yoko Sekita,* Yang Xi,* Kimi Araki,‡ Ken-ichi Yamamura,‡ Masanobu Oshima,§ Takaaki Ito,¶ Hideo Baba,† and Mitsuyoshi Nakao*

From the Departments of Medical Cell Biology, and Developmental Genetics,‡ Institute of Molecular Embryology and Genetics, Kumamoto University, Kumamoto; the Division of Genetics,§ Cancer Research Institute, Kanazawa University, Kanazawa; and the Departments of Gastroenterological Surgery,† and Pathology and Experimental Medicine,¶ Graduate School of Medical Sciences, Kumamoto University, Kumamoto, Japan*

The development of stomach cancer is closely associated with chronic inflammation, and the Wnt/β-catenin signaling pathway is activated in most cases of this cancer. High-mobility group A (HMGA) proteins are oncogenic chromatin factors that are primarily expressed not only in undifferentiated tissues but also in various tumors. Here we report that HMGA1 is induced by the Wnt/β-catenin pathway and maintains proliferation of gastric cancer cells. Specific knockdown of HMGA1 resulted in marked reduction of cell growth. The loss of β-catenin or its downstream *c-myc* decreased *HMGA1* expression, whereas Wnt3a treatment increased *HMGA1* and *c-myc* transcripts. Furthermore, Wnt3a-induced expression of *HMGA1* was inhibited by *c-myc* knockdown, suggesting that HMGA1 is a downstream target of the Wnt/β-catenin pathway. Enhanced expression of HMGA1 coexisted with the nuclear accumulation of β-catenin in about 30% of gastric cancer tissues. To visualize the expression of HMGA1 *in vivo*, transgenic mice expressing endogenous HMGA1 fused to enhanced green fluorescent protein were generated and then crossed with *K19-Wnt1/C2mE* mice, which develop gastric tumors through activation of both the Wnt and prostaglandin E2 pathways. Expression of HMGA1-enhanced green fluorescent protein was normally detected in the forestomach, along the upper border of the glandular stomach, but its expression was also up-regulated in cancerous glandular stomach. These data suggest that HMGA1 is involved in proliferation and gastric tumor formation via the Wnt/β-catenin pathway. *(Am J Pathol 2009, 175:1675–1685; DOI: 10.2353/ajpath.2009.090069)*

Gastric cancer is the second leading cause of human cancer deaths worldwide, and it is known to be closely associated with chronic inflammation caused by *Helicobacter pylori* infection.[1,2] This disease is an example of human oncogenesis that is etiologically induced by extrinsic or environmental factors. Despite preventive therapies and numerous efforts to identify premalignant lesions, gastric cancer is often diagnosed at the advanced stages.[3,4] It is therefore crucial to understand the molecular basis of gastric tumorigenesis to identify diagnostic and therapeutic targets in this cancer.

High-mobility group A proteins (HMGA1 and HMGA2, formerly HMGI/Y and HMGI/C, respectively) are non-histone, architectural chromatin proteins that participate in various cell regulation activities, including cell growth and proliferation.[5,6] HMGA1 and HMGA2 are encoded by two distinct genes, and are characterized by the presence of three DNA-binding motifs, named AT hooks, which preferentially bind stretches of AT-rich DNA sequences.[7] *HMGA* genes are highly expressed during embryonic development, whereas their expression is down-regulated in differentiated cells in adults,[8,9] though both *HMGA1* and *HMGA2* can be induced by mitogenic stimuli.[7,10] Notably, *HMGA* genes are frequently reactivated in many types of human cancer, and the overexpression of HMGA proteins is linked to malignant transformation and progression in human cancers, including

Supported by a Grant-in-Aid for Scientific Research on Priority Areas from the Ministry of Education, Culture, Sports, Science and Technology (M.N. and S.W.), and by a Grant-in-Aid for Global Center of Excellence, "Cell Fate Regulation Research and Education Unit," Kumamoto University.

Accepted for publication June 23, 2009.

Supplemental material for this article can be found on *http://ajp.amjpathol.org*.

Address reprint requests to Mitsuyoshi Nakao, M.D., Ph.D., Department of Medical Cell Biology, Institute of Molecular Embryology and Genetics, Kumamoto University, 2-2-1 Honjo, Kumamoto 860-0811, Japan. E-mail: mnakao@gpo.kumamoto-u.ac.jp.

gastric cancer.[11–14] In addition to the above reports, our recent study determined that HMGA2 maintains epithelial–mesenchymal transition in human pancreatic adenocarcinomas.[15] However, the biological roles of the different HMGA proteins in different cancer phenotypes, and the induction mechanism of oncogenic *HMGA* genes are largely unknown.

Among the cancer-related signaling pathways, the canonical Wnt pathway, also known as the Wnt/β-catenin pathway, is involved in gastrointestinal carcinogenesis. Wnt ligands engage their receptor complex, stabilize intracellular levels of β-catenin, and allow the nuclear accumulation of β-catenin, together with the transcription factor lymphoid enhancer-binding factor 1/ T cell-specific factor, followed by transcriptional activation of the Wnt/β-catenin target genes such as *c-myc* and *cyclin D*.[16] In the absence of Wnt, destruction complexes consisting of glycogen synthase kinase-3β, the adenomatous polyposis coli protein, and axin, bind and phosphorylate β-catenin, which is thus targeted for ubiquitination and proteolytic degradation. Constitutive activation of the Wnt/β-catenin pathway can occur due to mutations in the *adenomatous polyposis coli*, *β-catenin*, and *axin* genes during cancer development.[17–22] The nuclear localization of β-catenin is a hallmark of gastric cancer tissues.[23] It has been recently reported that *K19-Wnt1/C2mE* transgenic mice expressing Wnt1, cyclooxygenase-2 (COX2), and microsomal prostaglandin E synthase-1 in gastric epithelial cells, under the control of the *cytokeratin 19* (*K19*) gene promoter. They develop dysplastic stomach tumors, so providing an animal model of human gastric adenocarcinoma.[24] Interestingly, the activation of both Wnt and inflammation pathways was required for cancer development, since either altered pathway alone did not lead to tumor formation. Collectively, these observations suggest that the Wnt/β-catenin pathway is involved in gastric tumorigenesis, although the precise mechanisms remain undetermined.

During our investigations into chromatin factors, we found that HMGA1 is induced by the Wnt/β-catenin pathway and maintains proliferation of gastric cancer cells. Depletion of HMGA1 resulted in reduced cell proliferation. Wnt3a treatment increased *HMGA1*, as well as *c-myc* transcripts, and the Wnt3a-induced expression of *HMGA1* was inhibited by *c-myc* knockdown. Overexpression of HMGA1 was consistently correlated with the nuclear accumulation of β-catenin in human gastric cancer tissues. To visualize the Hmga1 protein *in vivo*, transgenic mice expressing endogenous Hmga1 fused to enhanced green fluorescent protein (EGFP) were generated and crossed with *K19-Wnt1/C2mE* mice. Expression of Hmga1-EGFP was normally found in the forestomach, along the upper border of the glandular stomach. In contrast, Hmga1-EGFP was up-regulated in cancerously proliferative glandular stomach. Based on the results of the present study, we discuss the role of HMGA1 in gastric tumor formation via the Wnt/β-catenin pathway.

Table 1. Small Interfering RNAs Used in this Study

Name	siRNA sequence
HMGA1 si-S	5′-GUGCCAACACCUAAGAGACCUTT-3′
HMGA1 si-AS	5′-AGGUCUCUUAGGUGUUGGCACTT-3′
HMGA1 si-S2	5′-GCAGGAAAAGGACGGCACUTT-3′
HMGA1 si-AS2	5′-AGUGCCGUCCUUUUCCUGCTT-3′
HMGA2 si-S	5′-CCGGUGAGCCCUCUCCUAATT-3′
HMGA2 si-AS	5′-UUAGGAGAGGGCUCACCGGTT-3′
c-myc si-S	5′-CUAUGACCUCGACUACGACTT-3′
c-myc si-AS	5′-GUCGUAGUCGAGGUCAUAGTT-3′
stealth c-myc-S	5′-UUUCAACUGUUCUCGUCGUUUCCGC-3′
stealth c-myc-AS	5′-GCGGAAACGACGAGAACAGUUGAAA-3′
β-catenin si-S	5′-CAGUCUUACCUGGACUCUGTT-3′
β-catenin si-AS	5′-CAGAGUCCAGGUAAGACUGTT-3′
GL3 si-S	5′-CUUACGCUGAGUACUUCGATT-3′
GL3 si-AS	5′-UCGAAGUACUCAGCGUAAGTT-3′

Materials and Methods

Cell Culture and Treatment

AGS, KATO-III, and Panc1 cells (American Type Culture Collection, Manassas, VA), as well as HEK293 cells (Health Science Research Resources, Osaka, Japan) were used. Two gastric cancer cell lines, HSC39 and HSC57, were a gift from Dr. K. Yanagihara and Dr. T. Ushijima (National Cancer Center Research Institute, Tokyo, Japan). The culture conditions were: RPMI-1640 medium (Sigma-Aldrich, St. Louis, MO) supplemented with 10% (v/v) heat-inactivated fetal bovine serum for AGS, HSC39, HSC57, and KATO-III cells; 1:1 mixture of Dulbecco's modified Eagle's minimum essential medium and Ham's F-12 nutrient medium supplemented with 10% fetal bovine serum for Panc1 cells; and low glucose Dulbecco's modified Eagle's minimum essential medium supplemented with 10% fetal bovine serum for HEK293 cells. AGS cells (1×10^5/well) were grown in 6-well plates and treated with 100 μmol/L NS-398 (Wako Pure Chemical Industries, Ltd., Osaka, Japan) or 100 μmol/L indomethacin (Wako Pure Chemical Industries, Ltd.) for 48 hours. Secreted Wnt3a was prepared from culture medium of L9 cells stably expressing Wnt3a, which were a gift from Dr. S. Takada (National Institutes of Natural Sciences, Okazaki, Japan). HEK293 cells were treated with 50% Wnt3a-condition medium for 48 hours.

Small Interfering RNA Mediated Knockdown

Small interfering (si)RNA duplexes were designed for targeting mRNAs encoding human HMGA1, HMGA2, β-catenin, and c-*myc* (Japan Bio Services Co., Ltd., Saitama, Japan), and are listed in Table 1. The selected siRNA sequences were submitted to human genome and Expressed Sequence Tags databases to ensure their target specificities. Validated stealth RNA interference against c-*myc* and its negative control was obtained from Invitrogen (Carsbad, CA). The siRNAs were transfected into the cells using Oligofectamine RNAiMAX (Invitrogen, Carsbad, CA).

Table 2. Oligonucleotides Used for the PCR

Name	Primer sequence
Human	
HMGA1 S	5′-TGAGTCCCGGGACAGCACTGGTAG-3′
HMGA1 AS	5′-GCGGCTAAGTGGGATGTTAGCCTTG-3′
HMGA2 S	5′-CAGGATGAGCGCACGCGGTGAGGGC-3′
HMGA2 AS	5′-CCATTTCCTAGGTCTGCCTCTTGGC-3′
c-myc S	5′-TCGTCTCAGAGAAGCTGGCCT-3′
c-myc AS	5′-CTTTTCCACAGAAACAACATCG-3′
β-catenin S	5′-CAGTTGCTTGTTCGTGCACAT-3′
β-catenin AS	5′-CAAGTCCAAGATCAGCAGTCTC-3′
GAPDH S	5′-GATGCCCCCATGTTCGT-3′
GAPDH AS	5′-CAGGGGTCTTACTCCTTGGA-3′
Mouse	
Hmga1 S	5′-ATGAGCGAGTCGGGCTCAAAG-3′
Hmga1 AS	5′-TCACTGCTCCTCCTCAGAG-3′
Gapdh S	5′-ATCACCATCTTCCAGGAGCGAG-3′
Gapdh AS	5′-GTTGTCATGGATGACCTTGGCC-3′

Cell Proliferation Analysis

Cell proliferation was assessed by seeding AGS, HSC57, and KATO-III cells (1×10^5/well) into 6-well plates. The cells were transfected with HMGA1, HMGA2, or control siRNAs (50 pmol) on day 0, using oligofectamine RNAiMAX, according to the manufacturer's protocols. The number of viable cells was counted using a hemocytometer. Data were obtained from three independent experiments.

Reverse Transcription and Quantitative Real-Time PCR

Two micrograms of the total RNAs were treated with DNase I (Roche Diagnostics, Mannheim, Germany) and reverse-transcribed using a High Capacity cDNA Reverse Transcription Kit (Applied Biosystems, Foster City, CA). PCR amplification was then performed using specific primers for the indicated transcripts (Tables 2 and 3). For quantification, real-time PCR analysis was performed using Power SYBR Green PCR Master Mix on an ABI Prism 7500 Sequence Detector (Applied Biosystems). PCR amplification was repeated at least three times from more than three independent experiments. The relative fold induction was quantified using the comparative threshold cycle method, and β-actin was used as a normalization control. Primer sets are listed in Table 3.

Plasmids and Luciferase Assay

The human HMGA1 promoter-luciferase construct (a generous gift from Dr. K. Peeters, University of Leuven, Belgium[25]) was introduced into HEK293 cells, together with phRL-SV40 (1 ng) (Promega, Madison, WI) using Fugene6 (Roche Diagnosics). Luciferase activities were checked 48 hours after transfection using the dual luciferase reporter assay system (Promega). Firefly luciferase activities were normalized to *Renilla* luciferase activities. Luciferase activities were determined from more than three independent assays.

Table 3. Oligonucleotides Used for the Quantitative Real-time PCR

Name	Primer sequence
Human	
HMGA1 S	5′-TCCAGGAAGGAAACCAAGG-3′
HMGA1 AS	5′-AGGACTCCTGCGAGATGC-3′
c-myc S	5′-TGCTCCATGAGGAGACACC-3′
c-myc AS	5′-CTTTTCCACAGAAACAACATCG-3′
β-catenin S	5′-GCTTTCAGTTGAGCTGACCA-3′
β-catenin AS	5′-CAAGTCCAAGATCAGCAGTCTC-3′
Cyclin D1 S	5′-GAAGATCGTCGCCACCTG-3′
Cyclin D1 AS	5′-GACCTCCTCCTCGCACTTCT-3′
YWHAZ S	5′-AGACGGAAGGTGCTGAGAAA-3′
YWHAZ AS	5′-TCAAGAACTTTTCCAAAAGAGACA-3′
β-actin S	5′-CCAACCGCGAGAAGATGA-3′
β-actin AS	5′-CCAGAGGCGTACAGGGATAG-3′
Mouse	
Hmga1 S	5′-CTCCAGGGAGGAAACCAAG-3′
Hmga1 AS	5′-CAGAGGACTCCTGGGAGATG-3′
Wnt1 S	5′-ACAGTAGTGGCCGATGGTG-3′
Wnt1 AS	5′-CTTGGAATCCGTCAACAGGT-3′
K19 S	5′-ATGAGATCATGGCCGAGAAG-3′
K19 AS	5′-GGTGTTCAGCTCCTCAATCC-3′
Ki67 S	5′-AGGGTAACTCGTGGAACCAA-3′
Ki67 AS	5′-TTAACTTCTTGGTGCATACAATGTC-3′
β-actin S	5′-CCAACCGTGAAAAGATGACC-3′
β-actin AS	5′-CCAGAGGCATACAGGGACAG-3′

Generation of Hmga1-EGFP *Knock-In Mice*

To generate *Hmga-1-EGFP* knock-in mice, 2.5- and 4-kb fragments containing the *Hmga1* gene were amplified by genomic PCR from mouse bacterial artificial chromosome clone RP23-189L19, derived from C57BL/6J mice. The *EGFP* gene was fused in-frame to the last open reading frame before the *Hmga1* translation stop codon in the 5′ homologous arm. A 2.5-kb 5′ arm of homology (EcoRI to BamHI) including exons 3, 4, and 5 before the stop codon fused *EGFP* gene, and a 4-kb 3′ arm of homology (XbaI/SpeI to *MluI*) including exon 5 after the stop codon, were cloned into 5′ and 3′ multiple-cloning sites of the pIRES-neo3 vector (Clontech Laboratories, Inc., Mountain View, CA) that lacked a synthetic intron. After sequence confirmation, the construct was linearized using *MluI* and introduced into wild-type TT2-KTPU8 F1 mouse embryonic stem (ES) cells by electroporation. The transfected ES cells were then cultured in selection medium containing 0.2 mg/ml G418. Southern blot analysis using a probe 5′ to the BamHI site was performed on G418 resistant colonies to identify the ES cells with correct incorporation of the targeting construct into the genome. The gene targeted ES cells were then aggregated with morulae of ICR mice. The aggregated embryos were transferred to pseudopregnant females and allowed to develop to term. The chimeric mice were bred with C57BL/6 wild-type mice, and the resulting pups were screened for the presence of the heterozygous targeted allele. The genotype of the mice was determined by Southern blot analysis and PCR of genomic DNA isolated from the tail or ear. Heterozygous mice were intercrossed to obtain homozygous mice. *Hmga1-EGFP/Hmga1-EGFP* mice were also crossed with *K19-Wnt1/C2mE* mice[24] or

C57BL/6 mice (as a control), to analyze the expression of *Hmga1-EGFP* in normal tissues and gastric tumors.

Immunohistochemistry

Mouse tissues were fixed in 4% paraformaldehyde and embedded in paraffin. Histological sections were cut at 3 μm. Human stomach tumor tissue arrays (BioChain Institute, Inc., Hayward, CA) or mouse tissue samples were deparaffinized, and antigens were retrieved by autoclaving at 120°C for 15 minutes for β-catenin and HMGA1, in a buffer solution (0.01 M/L sodium citrate [pH 6.0] for β-catenin, 1 mmol/L EDTA/PBS [pH 9.0] for HMGA1). The slides were then incubated in methanol with 0.3% hydrogen peroxide for 30 minutes to block endogenous peroxidase activity. Thereafter, tissue sections were immersed in 0.5% BlockAce (Dainippon Sumitomo Pharma Co., Ltd., Osaka, Japan) in PBS for 30 minutes, covered with primary antibodies, and incubated overnight at 4°C. To detect nuclear β-catenin, mouse monoclonal antibodies for the stabilized (active) form of β-catenin that is dephosphorylated on Ser-37 or Thr-41 (Clone 8E7; Upstate, Charlottesville, VA) were used as the primary antibodies.[24]. Goat polyclonal HMG-I(Y) antibodies (N-19; Santa Cruz Biotechnology, Inc., CA) were used to detect HMGA1, and rabbit polyclonal GFP antibodies (FL; Santa Cruz Biotechnology, Inc., CA) were used to detect GFP. As the internal positive control, anti-Sp1 antibodies were used (data not shown). Visualization of the immunoreactions was performed using Histofine Simple Stain MAX-PO (Nichirei Bioscience Inc., Tokyo, Japan) and 3,3-diaminobenzidine tetrahydrochloride (Dako, Glostrup, Denmark). The slides were counterstained with hematoxylin and mounted with Malinol (Muto Pure Chemicals Co., Ltd., Tokyo, Japan).

Carcinoma cells with moderate or strong nuclear HMGA1 staining were counted as HMGA1-positive, while cells with weak nuclear staining and/or diffuse cytoplasmic staining were counted as negative. Cells with nuclear β-catenin staining were judged as β-catenin-positive, and those with membrane-associated β-catenin or no β-catenin staining were counted as negative. Positive nuclear staining for HMGA1 or β-catenin was exemplified in adenocarcinoma. HMGA1-positive cells and β-catenin-positive cells were quantitatively assessed by counting carcinoma cells (mean, 233; range, 110 to 450) in the same tissue samples.

To observe fluorescent images, mouse tissues were fixed in 4% paraformaldehyde for 3 hours, incubated in 20% sucrose overnight, and frozen in Tissue-Tek optimal cutting temperature embedding compound (Sakura Finetechnical Co., Ltd., Tokyo, Japan). Embedded frozen tissues were sectioned at 5 μm.

Statistical Analysis

Statistical analyses were performed using JMP 7.0.1 for Windows software (SAS Institute Inc., Cary, NC). Significant differences in real-time PCR quantification were evaluated using two-tailed paired *t*-tests. The association between HMGA1-positive cells and β-catenin-positive cells was analyzed using Pearson's correlation coefficient, which varies from a perfect negative correlation (−1) to a perfect positive correlation (+1). Statistical significance was considered at a probability level of 0.05 or less.

Results

HMGA1 Maintains Proliferation of Gastric Cancer Cells in Association with β-Catenin

Several reports have shown that HMGA1 is overexpressed in gastric cancer,[13,26,27] but the precise role of HMGA1 in the malignant phenotype remains undetermined. To examine the expression status of *HMGA* genes in human gastric cancer cells, we performed reverse transcription (RT)-PCR (Figure 1A). *HMGA1* was expressed in all four gastric cancer cell lines (HSC39, HSC57, AGS, and KATO-III), whereas *HMGA2* expression was not detected in any of the gastric cancer cells studied. In normal stomach tissue, *HMGA1* was expressed at low levels, while *HMGA2* was not detected. As a control, both *HMGA1* and *HMGA2* transcripts were found in HEK293 and Panc1 cells. To test the effect of HMGA1 on cell proliferation, we used siRNAs against *HMGA1* or *HMGA2* transcripts, whose knockdown effects have been previously demonstrated at both the RNA and protein levels.[15] Western blot analysis showed that HMGA1 was expressed and depleted by the specific knockdown in AGS and HSC57 cells (Figure 1B). Quantitative RT-PCR analysis showed that *HMGA1* was equally down-regulated by two distinct siRNAs in AGS cells (Figure 1C), and in HSC57 and KATO-III cells (data not shown). Notably, the knockdown of *HMGA1* significantly reduced the growth rate of the gastric cancer cells studied, compared with the use of control and HMGA2 siRNAs. Cell death was assessed by fluorescence activated cell sorting analysis and was not increased under knockdown conditions (data not shown). These results indicate that HMGA1 is involved in maintaining the proliferation of the gastric cancer cells.

Nuclear localization of β-catenin, a hallmark of Wnt/β-catenin signaling activation, is found in approximately 30% to 50% of gastric cancer tissues and in many kinds of gastric cancer cell lines.[23,28] Our expression studies showed that transcripts for β-catenin and *c-myc*, known as key factors in the Wnt/β-catenin pathway, were expressed in the gastric cancer cells studied (Figure 1A). To assess the effect of the Wnt/β-catenin pathway on *HMGA1* expression, quantitative RT-PCR was performed following the selective knockdown of β-catenin or *c-myc* (Figure 1C). The depletion of either β-catenin or *c-myc* significantly reduced the expression of *HMGA1* ($P < 0.01$), as did HMGA1 knockdown. In addition, the loss of β-catenin also decreased *c-myc* and *cyclin D1* transcripts. Since the knockdown of β-catenin or *c-myc* reduced HMGA1 expression by approximately 50%, we examined whether other factors may mediate the transcriptional up-regulation of HMGA1. The use of COX2 inhibitors, NS-398 and indomethacin, decreased their

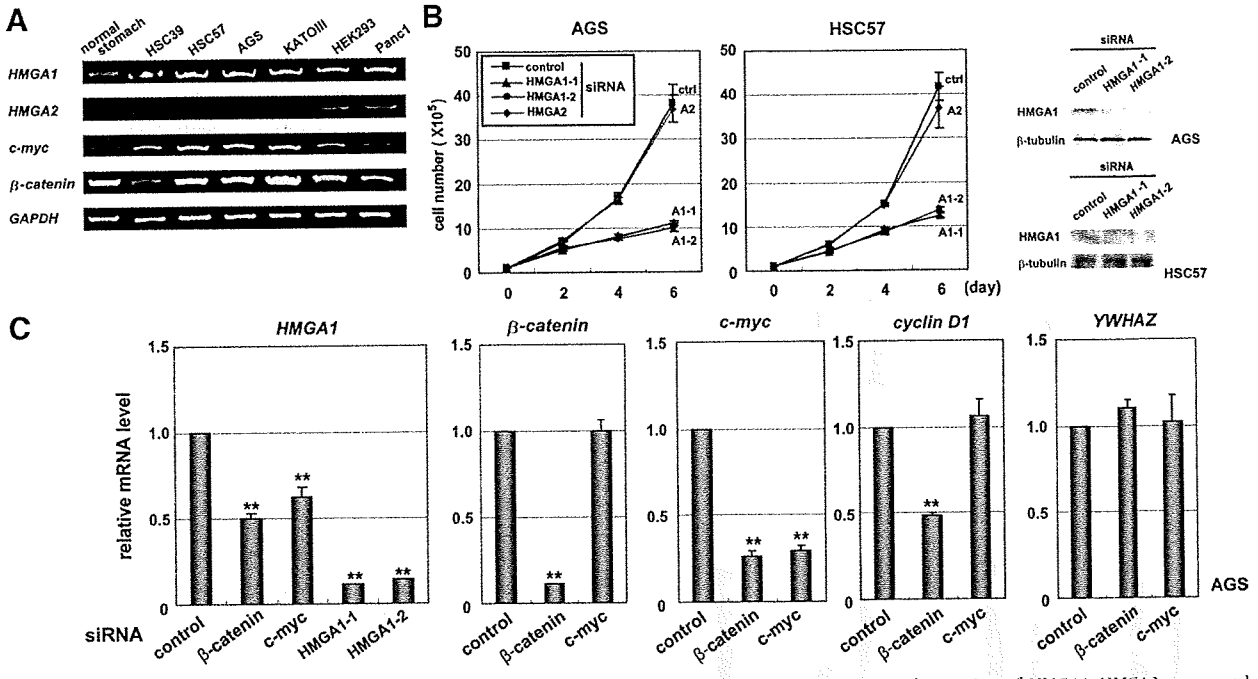

Figure 1. HMGA1 maintains proliferation of gastric cancer cells in association with β-catenin. **A:** Expression status of transcripts of *HMGA1*, *HMGA2*, *c-myc*, and *β-catenin* in human gastric cancer cells. RT-PCR was performed using *glyceraldehyde-3-phosphate dehydrogenase* (*GAPDH*) as a control. Gastric cancer cell lines are HSC39, HSC57, AGS, and KATO-III. Normal stomach tissue, HEK293 cells, and Panc1 pancreatic cancer cells are used as controls. **B:** Effect of *HMGA1* and *HMGA2* knockdown on cell proliferation. The cell numbers were determined on days 0, 2, 4, and 6 after the small interfering (si)RNA-mediated knockdown. The knockdown efficiencies with individual siRNAs are shown in the **right panel** and in **C** (**left panel**). Results were obtained from three independent experiments. Error bars indicate SD. **C:** Effect of *β-catenin* and *c-myc* knockdown on *HMGA1* expression. Quantitative RT-PCR was performed in *β-catenin* and *c-myc*-knockdown AGS cells. The relative mRNA levels with the use of control siRNAs were normalized to 1. *cyclin D1* and tyrosine 3-monooxygenase/tryptophan 5-monooxygenase activation protein, zeta polypeptide (*YWHAZ*) genes were used as controls. Values are given as means and standard deviations from more than three independent experiments. $^{**}P < 0.01$ when compared with control cells.

proliferation but did not affect *HMGA1* expression in AGS cells, suggesting that COX2 pathway unlikely influences on the expression of *HMGA1* (data not shown). These results suggest that HMGA1 is involved in maintaining the growth activities of the gastric cancer cells, by acting as a downstream target of the Wnt/β-catenin pathway.

c-myc *Induces* HMGA1 *Expression in the Wnt/β-Catenin Pathway*

We used HEK293 cells that have no constitutive Wnt/β-catenin activation but accumulate nuclear β-catenin after treatment with Wnt3a[29,30] to investigate how the Wnt/β-catenin pathway induced the expression of *HMGA1*. We used a luciferase reporter assay in HEK293 cells (Figure 2A) to examine the transcriptional role of Wnt/β-catenin in the human *HMGA1* gene promoter. An E-box motif in the *HMGA1* gene promoter (at position −1353 from the transcriptional start site) has been reported to bind *c-myc*,[10,31] and we therefore used a reporter plasmid containing the promoter region (nucleotides −1745 to +265) upstream of the luciferase gene. Treatment of the cells with Wnt3a increased the *HMGA1* promoter activity by about twofold, while the depletion of *c-myc* reduced the luciferase activity relative to the control. These data suggest that the *HMGA1* promoter can be induced by Wnt3a and *c-myc*. Under Wnt3a treatment, we then measured the mRNA levels of endogenous *HMGA1* in HEK293 cells, using quantitative RT-PCR analysis (Figure 2B). Wnt3a up-regulated the expression of the *HMGA1* and *c-myc* genes ($P < 0.01$). In addition, *c-myc* knockdown reduced the expression of *HMGA1* ($P < 0.01$) (Figure 2C), suggesting that *c-myc* mediates *HMGA1* expression. We treated the *c-myc* knockdown cells with Wnt3a to determine whether *c-myc* is required for Wnt3a-induced *HMGA1* expression (Figure 2D). The depletion of *c-myc* reduced *HMGA1* expression in the control cells and inhibited *HMGA1* induction in Wnt3a-treated cells. The reduction of *HMGA1* by the knockdown of *c-myc* was found in Wnt3a-untreated cells as well as Wnt3a-treated cells, suggesting that *c-myc* maintains the basal levels of *HMGA1* expression. Collectively, these data suggest that the expression of *HMGA1* is positively controlled at least in part via the Wnt/β-catenin/*c-myc* pathway.

Correlation between HMGA1 and β-Catenin Expression in Human Gastric Cancer Tissues

To investigate the involvement of HMGA1 in Wnt/β-catenin signaling *in vivo*, we examined 64 primary gastric carcinoma tissues, using immunohistochemical techniques (Figure 3). Representative images are shown in Figure 3A, and the data for each tissue are summarized in Supplemental Table 1[32] at *http://ajp.amjpathol.org*. Nuclear accumulation of HMGA1 and β-catenin was found in gastric adenocarcinomas (Figure 3D–F), but not in

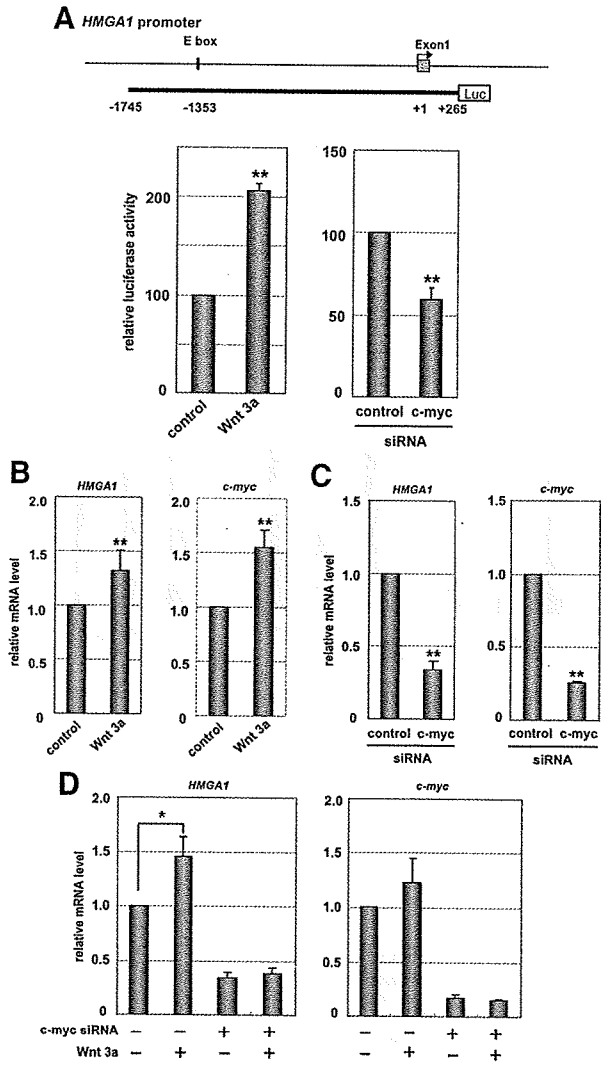

Figure 2. The wnt/β-catenin/*c-myc* pathway induces expression of *HMGA1*. **A:** Effect of Wnt3a and *c-myc* knockdown on human *HMGA1* gene promoter. The human *HMGA1* promoter (the region from −1745 to + 265 from the transcriptional start site, containing the E box that binds *c-myc*-luciferase construct[25] was introduced into HEK293 cells, together with phRL-SV40 (1 ng). Luciferase activities were checked 48 hours after transfection using the dual luciferase reporter assay. Luciferase activities of the control were normalized to 100. $^{**}P < 0.01$ when compared with control cells. **B–D:** Expression of endogenous *HMGA1* and *c-myc* genes. Quantitative reverse transcription-polymerase chain reaction (RT-PCR) analysis of *HMGA1* and *c-myc* transcripts in HEK293 cells was performed using Wnt3a-treatment (**B**), *c-myc* knockdown (**C**), and a combination of Wnt3a and *c-myc* knockdown (**D**). The depletion of *c-myc* inhibited Wnt3a-induced *HMGA1* expression. The relative control mRNA levels were normalized to 1. Values are given as means and standard deviations from more than three independent experiments. Asterisks indicate statistically significant differences compared with control cells ($^{*}P < 0.05$, $^{**}P < 0.01$).

normal stomach tissues (Figure 3A, A–C). High HMGA1 expression was found in 36 out of the 64 gastric carcinomas studied (56.3%), where HMGA1 was densely stained in the nuclei of more than 30% of the cancer cells (Figure 3G). Similarly, β-catenin was highly expressed in 23 out of 64 cancer tissues (35.9%), where nuclear β-catenin was detected in more than 30% of the cancer cells. As in Figure 3D–F, high expression of both HMGA1 and β-catenin was observed in nine carcinoma tissue samples. To assess the correlation between HMGA1 and β-catenin expression, we compared the percentages of HMGA1-positive cells and nuclear β-catenin-positive cells in the same samples (Figure 3H) and analyzed the results using Pearson's correlation coefficient analysis. There was a positive correlation between HMGA1-positive and β-catenin-positive cells in the gastric cancer tissues ($r = 0.54$, $P < 0.0001$). In addition, there was no significant correlation of the expression status of HMGA1 or β-catenin with the histological type of gastric cancers (Supplemental Table 1[32] at *http://ajp.amjpathol.org*). These results suggest that enhanced expression of HMGA1 is correlated with Wnt/β-catenin signaling in naturally occurring gastric cancer.

Generation of Hmga1-EGFP Knock-In Mice

To visualize the expression of Hmga1 *in vivo*, we generated knock-in mice harboring the *Hmga1* gene fused to the *EGFP* gene (*Hmga1-EGFP*). The mouse *Hmga1* gene has five exons (Figure 4A), and *EGFP*-IRES-neo was inserted into exon 5 of the *Hmga1* gene in-frame, together with a deletion of the stop codon of the gene, through homologous recombination. The targeted knock-in allele resulted in expression of the *Hmga1-EGFP* fusion gene, driven by the endogenous promoter. After mouse ES cells were transfected with the targeting vector and selected by EGFP-positive and neomycin selection, we confirmed the occurrence of the expected homologous recombination in the cells by Southern blot analysis (Figure 4B). We obtained heterozygous mice (*Hmga1-EGFP/wild-type*), and then homozygous mice (*Hmga1-EGFP/Hmga1-EGFP*), as indicated in Figures 4C and 4D. A fluorescent macroscopic analysis of adult mice revealed that Hmga1-*EGFP* was markedly expressed in testis, cerebrum (Cx), cerebellum (Ce), Payer's patch (P), thymus, and spleen (Figure 4E). Low levels of Hmga1-*EGFP* were found in the kidney and liver (data not shown). In the stomach, it was of interest that Hmga1-*EGFP* was highly detected in the forestomach (Fs), but not in the glandular stomach (Gls), which is homologous to human stomach tissue. These observations not only agreed with a previous report on *Hmga1* mRNA levels in tissues,[33] but also determined the distribution of Hmga1 in specific parts of living tissues and organs.

Tumor-Associated Expression of HMGA1 in K19-Wnt1/C2mE/Hmga1-EGFP *Mice*

K19-Wnt1/C2mE transgenic mice have been reported to simultaneously overexpress Wnt1, COX-2, and prostaglandin E synthase-1 in gastric epithelial cells under the control of the *K19* gene promoter, which is transcriptionally active in the gastric epithelium,[24] resulting in the development of dysplastic gastric tumors at the upper glandular stomach, with similar histology to human gastric adenocarcinomas. We examined the expression status of *Hmga1* in *K19-Wnt1/C2mE* mice using RT-PCR and found that it was highly expressed in stomach tumors in these mice, compared with age-matched and non-can-

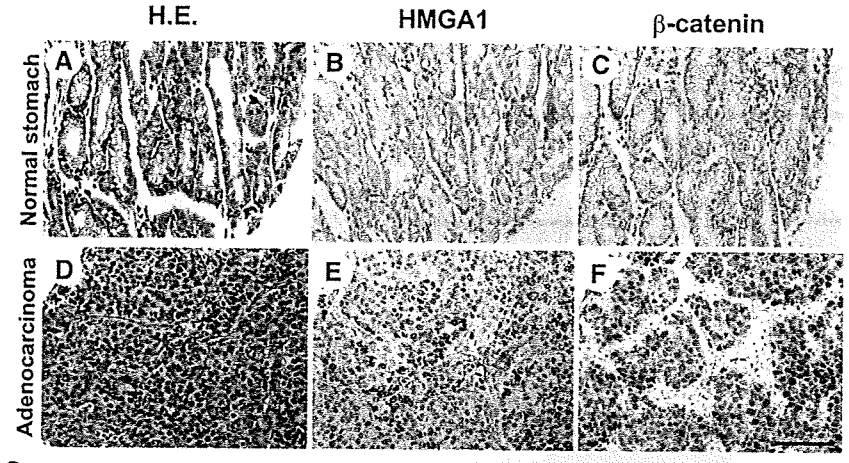

G

Positive cells(%)	Nuclear β-catenin	HMGA1
≧30	23	36
<30	41	28
Total	64	64

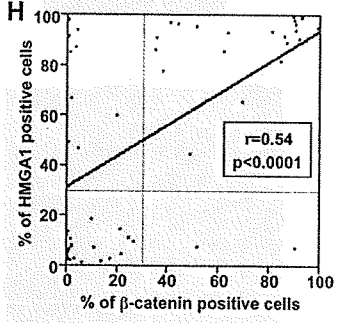

Figure 3. Correlation between HMGA1 and β-catenin expression in human gastric cancer tissues. Serial sections of normal stomach (**A–C**) and gastric adenocarcinoma (**D–F**). Normal and noncancerous tissues showed very weak staining for HMGA1 and nuclear β-catenin. In contrast, HMGA1 and β-catenin were highly accumulated in the nuclei of cancer cells. H&E staining (**A, D**), immunostaining for HMGA1 (**B, E**), and nuclear β-catenin (**C, F**). Scale bar = 100 μm. **G:** Percentage of HMGA1-positive cells and β-catenin-positive cells in gastric cancer tissues. High expression of HMGA1 was found in 36 out of 64 (56.3%) human primary gastric carcinomas studied, where HMGA1 was densely stained in the nuclei of more than 30% of the cancer cells. Nuclear expression of β-catenin was detected in 23 out of 64 cancer tissues (35.9%), where nuclear β-catenin was stained in more than 30% of the cancer cells. **H:** Percentage correlations between HMGA1-positive cells and β-catenin-positive cells in gastric cancer tissues. HMGA1-positive cells and β-catenin-positive cells were counted in the same samples (mean, 233; range, 110 to 450). Data were analyzed using Pearson's correlation coefficient. Supplemental Table S1[32] at *http://ajp.amjpathol.org* shows a summary of tumor grade and stage and the immunohistochemical data.

cerous glandular stomach controls (*$P < 0.05$ and **$P < 0.01$) (Figure 5A). We also determined the levels of *Hmga1* expression in the forestomach, glandular stomach, and tumors, using quantitative RT-PCR (Figure 5B). The mRNA levels of *Hmga1* in the forestomach showed no significant differences between wild-type and *K19-Wnt1/C2mE* mice, and were normalized to 1, based on more than three independent experiments. In wild-type mice, the expression levels of *Hmga1* in the glandular stomach were about 50% lower than those in the forestomach. In contrast, the expression of *Hmga1* was increased in the glandular stomach in *K19-Wnt1/C2mE* mice ($P < 0.01$). Moreover, *Hmga1* expression was markedly increased in the tumor tissues ($P < 0.01$). In addition to *Hmga1* induction, *Wnt1* and *cytokeratin 19* (*K19*) were also highly expressed in the glandular stomach and the tumors ($P < 0.01$). The expression level of endogenous *Wnt1*, which was detected by the 3′ untranslated region of the mRNAs, did not increase in *K19-Wnt1/C2mE* mice (data not shown). Further, the expression of *cyclin D1* and the proliferation marker *Ki-67* significantly increased in the glandular stomach and the tumors ($P < 0.01$), suggesting the hyperproliferative state in these tissues. Nuclear localization of β-catenin was mostly found in the tumors (data not shown, and[24]). Furthermore, tumor formation and invasion into the smooth muscle layers was observed histologically in *K19-Wnt1/C2mE* mice at 50 weeks of age (Figure 5C).

To visualize Hmga1 expression *in vivo*, we mated *K19-Wnt1/C2mE* mice with *Hmga1-EGFP* mice and investigated whether the development of gastric tumors was related to Hmga1 expression in the *K19-Wnt1/C2mE* mice using fluorescent macroscopic analysis (Figure 5D). As in the *Hmga1-EGFP* mice, Hmga1-*EGFP* expression was found in the forestomach, rather than the glandular stomach, in the *K19-Wnt1/C2mE/Hmga1-EGFP* mice. In contrast, tumor tissues raised in the glandular stomach of the *K19-Wnt1/C2mE/Hmga1-EGFP* mice showed increased expression of Hmga1-*EGFP* at 30 and 50 weeks of age. These observations demonstrated the oncogenic induction of Hmga1 *in vivo*, and were consistent with the mRNA levels of *Hmga1* found in the forestomach, glandular stomach and tumor tissues (Figure 5B). With fluorescence microscopy using sliced tissues, we further analyzed the expression of Hmga1-*EGFP* at the cellular level (Figure 5E). Hmga1-*EGFP* signals, as well as 4,6-diamidino-2-phenylindole-stained nuclei, were detected in the forestomach, especially along the upper border of the glandular stomach, in *Hmga1-EGFP* mice at 30 weeks of age, while most of tumor cells emerging in the upper glandular stomach showed Hmga1-*EGFP* expression in *K19-Wnt1/C2mE/Hmga1-EGFP* mice (See Discussion).

To confirm the induction of HMGA1 by the Wnt/β-catenin pathway *in vivo*, we finally examined the expression of Hmga1-*EGFP* in *K19-Wnt1/Hmga1-EGFP* mice with *K19* promoter-induced expression of Wnt1 alone (Figure 5F). *K19-Wnt1* mice had the expansion of undifferentiated progenitor cell population in the glandular stomach but did not show the dysplastic tumors in stomach.[2-4] An immunohistochemical analysis using anti-GFP antibodies demonstrated enhanced expression of Hmga1-*EGFP* at the middle and lower fundic glands in the glandular stomach of these mice. Collec-

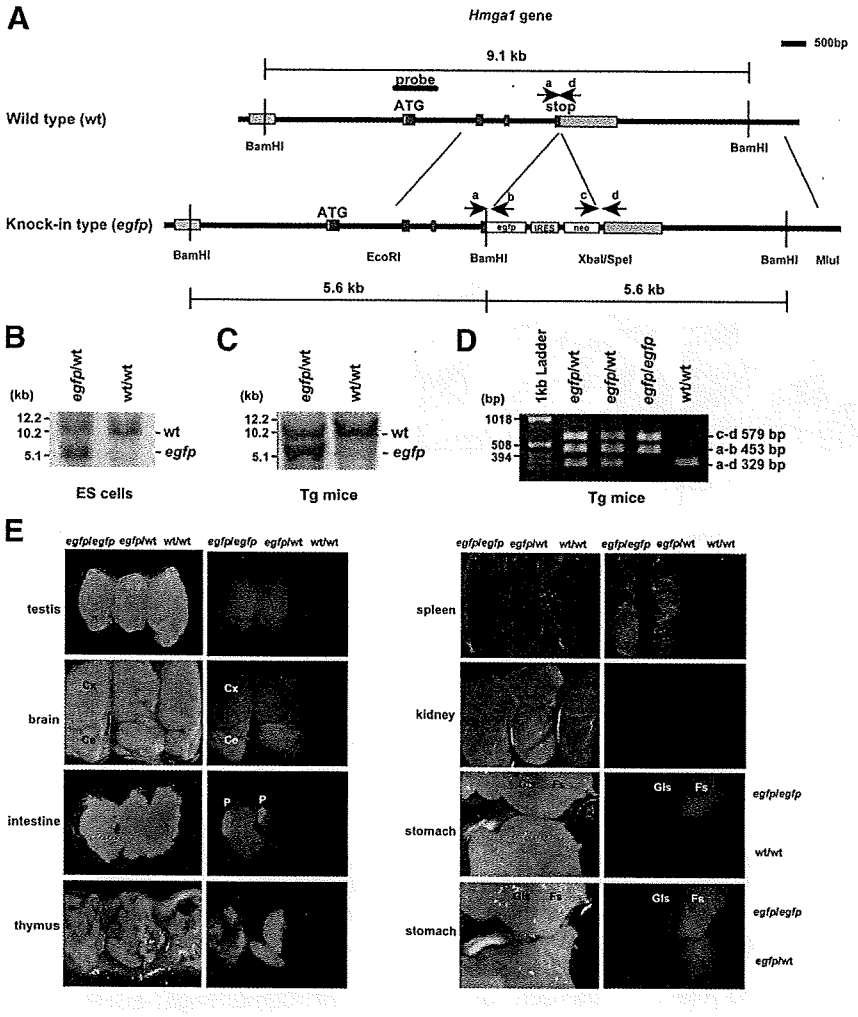

Figure 4. Characterization of *Hmga1-EGFP* knock-in mice. **A:** Generation of *Hmga1-EGFP* knock-in mice. Schematic representation of the mouse *Hmga1* gene locus and targeting construct are shown. In the knock-in type allele (*EGFP*), a 2.5-kb 5′ arm of homology (EcoRI to BamHI) containing exons 3, 4, and 5 before the stop codon was fused to the *EGFP* gene, IRES and *neo* sequences linked to a 4-kb 3′ arm of homology (XbaI/SpeI to *MluI*) containing exon 5 after the stop codon. **B:** Southern blot analysis using the indicated probe was performed to identify the embryonic stem (ES) cells that had correctly incorporated the targeting construct into the genome. **C, D:** The genotype of the *Hmga1-EGFP* knock-in mice was determined by Southern blot analysis (**C**) and polymerase chain reaction (**D**) of genomic DNAs using specific primers (**a:** 5′-TCATCCCCCTTTTGCAGAGG-3′, **b:** 5′-CGCTCCTGGACGTAGCCTTC-3′, **c:** 5′-TACCTGCCCATTCGACCACC-3′, **d:** 5′-ACAGGGACTGAGCCGAATCC-3′). **E:** Expression of Hmga1-*EGFP* protein in the knock-in mice. Fluorescent macroscopic analysis demonstrated the expression of Hmga1-*EGFP* in testis, cerebrum (Cx), cerebellum (Ce), Payer's patch (P), thymus, spleen, kidney and forestomach (Fs), but not in kidney and glandular stomach (Gls). Homozygous (*EGFP/EGFP*), heterozygous (*EGFP*/wt), and wild-type (w/w) mice are indicated.

tively, these results suggest that HMGA1 expression is induced by the Wnt/β-catenin pathway and maintains the proliferation of gastric tumor cells.

Discussion

Although gastric cancer is one of the most common malignancies, the molecular basis of its oncogenesis remains to be elucidated. The present study revealed that activation of the Wnt/β-catenin pathway induces HMGA1 expression through *c-myc*, resulting in the maintenance of proliferation of gastric cancer cells. Our data indicate that: (i) HMGA1 promotes proliferation of gastric cancer cells, (ii) Wnt/β-catenin signaling induces expression of HMGA1, depending on *c-myc*, (iii) a correlation between HMGA1-positive cells and β-catenin-positive cells exists in human gastric cancer tissues, (iv) *Hmga1-EGFP* knock-in mice visualize endogenous Hmga1 expression in the forestomach, rather than the glandular stomach, and (v) *K19-Wnt1/C2mE/Hmga1-EGFP* mice show that the expression of Hmga1 coexists with high levels of *Wnt1* in cancerous glandular stomach. These findings suggest that HMGA1 expression plays an important role in the maintenance of proliferative activities and tumor formation in gastric cancer.

Previous studies reported that HMGA1 was overexpressed in a broad range of human cancers, including gastric cancer,[13,26,27] and that it correlated with the occurrence of metastasis and poor prognoses.[11,12,14] We showed that HMGA1, but not HMGA2, was expressed in the gastric cancer cells studied, and that the depletion of HMGA1 significantly reduced the growth of these cells, suggesting that HMGA1 is involved in their proliferation. Despite the increasing evidence implicating HMGA1 in cancer development and progression, the molecular mechanisms of *HMGA1* reactivation in malignant changes remain undetermined. Several factors responsible for the induction of *HMGA1* expression have been identified, including serum, epidermal growth factor, fibroblast growth factor, hypoxia, and oncogenic Ras, in addition to transcription factors such as AP-1, *c-myc* and N-myc, which directly target the *HMGA1* promoter.[7,10,25,33,34] Our data first demonstrate that the Wnt/β-catenin pathway is linked to *HMGA1* induction, leading to proliferation, in human gastric cancer. The Wnt/β-catenin pathway positively controls *HMGA1* gene at least in part via

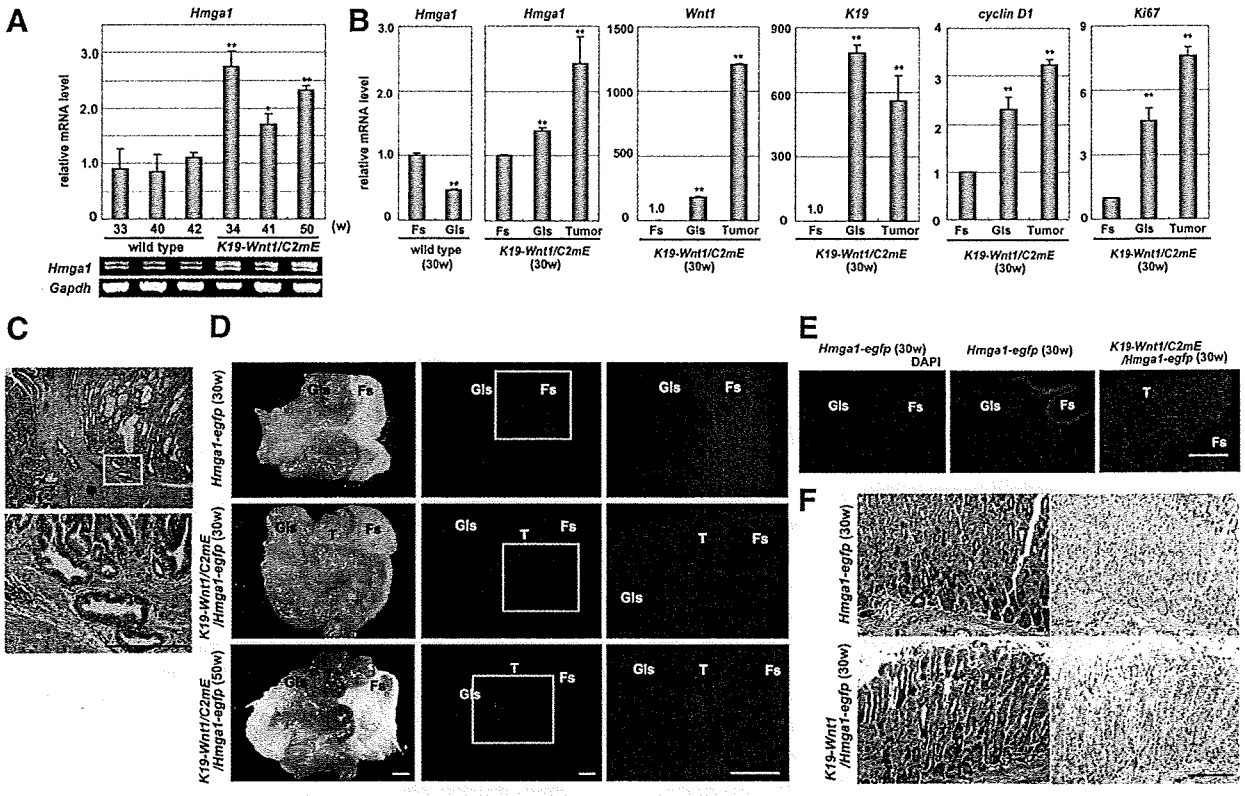

Figure 5. Tumor-associated expression of *Hmga1* in *K19-Wnt1/C2mE/Hmga1-EGFP* mice. **A:** Expression of *Hmga1* in mouse stomach tissues. RT-PCR analysis of *Hmga1* was performed using stomach and tumors from age-matched wild-type and *K19-Wnt1/C2mE* mice. The relative mRNA levels in wild-type mice (33w) were normalized to 1. $^{*}P < 0.05$, $^{**}P < 0.01$ when compared with control cells. **B:** Expression of *Hmga1* in the forestomach, glandular stomach, and tumor. Using quantitative RT-PCR, the mRNA levels of *Hmga1* in the forestomach (Fs) were normalized to 1. Expression of *Wnt1*, *cytokeratin 19* (*K19*), *cyclin D1*, and *Ki-67* was also shown. $^{**}P < 0.01$ when compared with control cells. **C:** H&E staining of stomach tumors in *K19-Wnt1/C2mE* mice at 50 weeks of age. The dysplastic tumors invaded into the smooth muscle layers. Scale bar = 100 μm. **D:** Induced expression of Hmga1-*EGFP* in tumor tissues. Fluorescent macroscopic analysis of the stomach tissues from *Hmga1-EGFP* mice at 30 weeks of age, and *K19-Wnt1/C2mE/Hmga1-EGFP* mice at 30 and 50 weeks of age was performed. Scale bar = 1 mm. The indicated region is magnified in the right panel. **E:** Expression of Hmga1-*EGFP* in the forestomach close to the glandular stomach and in most tumor cells. Frozen samples of the stomach from *Hmga1-EGFP* mice and *K19-Wnt1/C2mE/Hmga1-EGFP* mice were examined by fluorescence microscopy. Scale bar = 100 μm. **F:** Expression of Hmga1-*EGFP* in non-cancerous glandular stomach from *K19-Wnt1/Hmga1-EGFP* mice. H&E staining (left) and immunostaining of Hmga1-*EGFP* (right) of the glandular stomach from *Hmga1-EGFP* mice and *K19-Wnt1/Hmga1-EGFP* mice at 30 weeks of age. Scale bar = 100 μm.

c-myc. In addition, other factors may mediate the transcriptional up-regulation of *HMGA1*. As shown in Figure 2D, *c-myc* was involved in maintaining *HMGA1* expression in the absence of Wnt3a. The high expression of HMGA1 in some patients completely lacked nuclear β-catenin expression in the gastric cancers (Figure 3C). For these reasons, we checked whether the COX2 signaling is involved in *HMGA1* regulation. However, the use of COX2 inhibitors had little effect on *HMGA1* expression in gastric cancer cells (data not shown). On the other hand, we recently reported that HMGA2, but not HMGA1, is involved in the maintenance of oncogenic RAS-induced epithelial–mesenchymal transition in human pancreatic cancer cells.[15] This may be related with the fact that HMGA2 is primarily expressed in undifferentiated tissues of mesenchymal origin. Specific knockdown of HMGA2 inhibited proliferation of pancreatic cancer cells, notably leading to a transition to the epithelial state by up-regulation of E-cadherin. HMGA2 was induced by the oncogenic RAS pathway in pancreatic cancer, while this is not the case of gastric cancer. Thus HMGA proteins are likely to be induced by oncogenic pathways and contribute to malignant phenotypes in a cancer-specific manner.

The functional activation of Wnt/β-catenin may be responsible for gastrointestinal tumorigenesis,[35–37] where *c-myc* and cyclin D are key downstream effectors of the canonical Wnt pathway. Mutations of the *adenomatous polyposis coli, axin,* and *β-catenin* genes are common in colorectal cancer, and alterations of the *E-cadherin* gene occur in familial gastric cancer.[38] To demonstrate that HMGA1 is a downstream factor in the Wnt/β-catenin/*c-myc* pathway in gastric cancer cells, we showed that *HMGA1* was induced by Wnt3a in proliferating cells, and that there was a close correlation between the expression of HMGA1 and β-catenin in gastric cancer tissues. In *K19-Wnt1/Hmga1-EGFP* mice, Hmga1 expression in the proliferative glandular stomach also increased during the overexpression of *Wnt1* alone. Thus the expression of HMGA1 via the Wnt/β-catenin pathway may be one of the common mechanisms in oncogenesis. Since both Wnt/β-catenin and HMGA1 are actively expressed during organogenesis, these proteins would have an essential role in gut development, as well as tumorigenesis.

HMGA1 has previously been reported to be expressed during embryogenesis, whereas it has shown negligible expression in normal adult tissues.[7] Our investigations using *Hmga1-EGFP* mice, however, detected Hmga1 in

specific adult tissues, including the testis, brain, Payer's patch, thymus, spleen, and forestomach, together with the very low expression in the kidney and liver. This is the first mouse model that can visualize the expression of endogenous Hmga1 in living tissues and organs. Although dominantly expressed during embryogenesis, this protein may retain a biological function during the postnatal and adult stages. Indeed, it was reported that HMGA1 is required for T cell differentiation through the regulation of interleukin-2 and interleukin-2 receptor α-chain expression,[39–41] which may be related to its expression in lymphoid tissues in *Hmga1-EGFP* knock-in mice.

In this study, Hmga1-*EGFP* was densely detected in the forestomach, especially along the upper boundary of the glandular stomach, in *Hmga1-EGFP* mice. Previous and our studies showed that *K19-Wnt1/C2mE* mice usually develop dysplastic tumors in the proximal glandular stomach, close to the boundary with the forestomach.[24] There is the possibility that a cancer-initiated microenvironment is present in the proximal glandular stomach near the forestomach, where epithelial cells and the surrounding interstitial cells substantially transit and are exposed to the gastric acid. Since Hmga1 inhibits the retinoblastoma protein, leading to the activation of E2F-target genes,[42] Hmga1 may be likely implicated in the tumor development. Epithelial cells in the glandular stomach were also reported to exhibit intermediate characteristics between those of the forestomach and the duodenum in response to growth factors.[43] *Hmga1-EGFP* knock-in mice will prove useful for further investigations into the tissue-specific function of Hmga1 and the role of this protein in cancer and stem cell biology.

Acknowledgments

We thank Dr. Takaya Ichimura (Graduate School of Medical Sciences, Kumamoto University) for immunohistochemistry, Dr. Shinji Takada (National Institutes of Natural Sciences, Japan) for the L9 cells stably expressing Wnt3a, Dr. Kristel Peeters (University of Leuven, Belgium) for the human HMGA1 promoter-luciferase construct, and members of our laboratory for helpful discussions.

References

1. Parkin DM, Bray F, Ferlay J, Pisani P: Global cancer statistics, 2002. CA Cancer J Clin 2005, 55:74–108
2. Ushijima T, Sasako M: Focus on gastric cancer. Cancer Cell 2004, 5:121–125
3. Kapadia CR: Gastric atrophy, metaplasia, and dysplasia: a clinical perspective. J Clin Gastroenterol 2003, 36:S29–S36
4. Clouston AD: Timely topic: premalignant lesions associated with adenocarcinoma of the upper gastrointestinal tract. Pathology 2001, 33:271–277
5. Sgarra R, Rustighi A, Tessari MA, Di Bernardo J, Altamura S, Fusco A, Manfioletti G, Giancotti V: Nuclear phosphoproteins HMGA and their relationship with chromatin structure and cancer. FEBS Lett 2004, 574:1–8
6. Fusco A, Fedele M: Roles of HMGA proteins in cancer. Nat Rev Cancer 2007, 7:899–910
7. Reeves R: Molecular biology of HMGA proteins: hubs of nuclear function. Gene 2001, 277:63–81
8. Zhou X, Benson KF, Ashar HR, Chada K: Mutation responsible for the mouse pygmy phenotype in the developmentally regulated factor HMGI-C. Nature 1995, 376:771–774
9. Chiappetta G, Avantaggiato V, Visconti R, Fedele M, Battista S, Trapasso F, Merciai BM, Fidanza V, Giancotti V, Santoro M, Simeone A, Fusco A: High level expression of the HMGI (Y) gene during embryonic development. Oncogene 1996, 13:2439–2446
10. Wood LJ, Mukherjee M, Dolde CE, Xu Y, Maher JF, Bunton TE, Williams JB, Resar LM: HMG-I/Y, a new *c-myc* target gene and potential oncogene. Mol Cell Biol 2000, 20:5490–5502
11. Abe N, Watanabe T, Masaki T, Mori T, Sugiyama M, Uchimura H, Fujioka Y, Chiappetta G, Fusco A, Atomi Y: Pancreatic duct cell carcinomas express high levels of high mobility group I(Y) proteins. Cancer Res 2000, 60:3117–3122
12. Reeves R, Edberg DD, Li Y: Architectural transcription factor HMGI(Y) promotes tumor progression and mesenchymal transition of human epithelial cells. Mol Cell Biol 2001, 21:575–594
13. Nam ES, Kim DH, Cho SJ, Chae SW, Kim HY, Kim SM, Han JJ, Shin HS, Park YE: Expression of HMGI(Y) associated with malignant phenotype of human gastric tissue. Histopathology 2003, 42:466–471
14. Evans A, Lennard TW, Davies BR: High-mobility group protein 1(Y): metastasis-associated or metastasis-inducing? J Surg Oncol 2004, 88:86–99
15. Watanabe S, Ueda Y, Akaboshi S, Hino Y, Sekita Y, Nakao M: HMGA2 maintains oncogenic RAS-induced epithelial-mesenchymal transition in human pancreatic cancer cells. Am J Pathol 2009, 174:854–868
16. Peifer M, Polakis P: Wnt signaling in oncogenesis and embryogenesis—a look outside the nucleus. Science 2000, 287:1606–1609
17. Klaus A, Birchmeier W: Wnt signalling and its impact on development and cancer. Nat Rev Cancer 2008, 8:387–398
18. Clevers H: Wnt/β-catenin signaling in development and disease. Cell 2006, 127:469–480
19. Reya T, Clevers H: Wnt signalling in stem cells and cancer. Nature 2005, 434:843–850
20. Polakis P: Wnt signaling and cancer. Genes Dev 2000, 14:1837–1851
21. Satoh S, Daigo Y, Furukawa Y, Kato T, Miwa N, Nishiwaki T, Kawasoe T, Ishiguro H, Fujita M, Tokino T, Sasaki Y, Imaoka S, Murata M, Shimano T, Yamaoka Y, Nakamura Y: AXIN1 mutations in hepatocellular carcinomas, and growth suppression in cancer cells by virus-mediated transfer of AXIN1. Nat Genet 2000, 24:245–250
22. Liu W, Dong X, Mai M, Seelan RS, Taniguchi K, Krishnadath KK, Halling KC, Cunningham JM, Boardman LA, Qian C, Christensen E, Schmidt SS, Roche PC, Smith DI, Thibodeau SN: Mutations in AXIN2 cause colorectal cancer with defective mismatch repair by activating β-catenin/TCF signalling. Nat Genet 2000, 26:146–147
23. Clements WM, Wang J, Sarnaik A, Kim OJ, MacDonald J, Fenoglio-Preiser C, Groden J, Lowy AM: β-Catenin mutation is a frequent cause of Wnt pathway activation in gastric cancer. Cancer Res 2002, 62:3503–3506
24. Oshima H, Matsunaga A, Fujimura T, Tsukamoto T, Taketo MM, Oshima M: Carcinogenesis in mouse stomach by simultaneous activation of the Wnt signaling and prostaglandin E2 pathway. Gastroenterology 2006, 131:1086–1095
25. Cleynen I, Huysmans C, Sasazuki T, Shirasawa S, Van de Ven W, Peeters K: Transcriptional control of the human high mobility group A1 gene: basal and oncogenic Ras-regulated expression. Cancer Res 2007, 67:4620–4629
26. Xiang YY, Wang DY, Tanaka M, Suzuki M, Kiyokawa E, Igarashi H, Naito Y, Shen Q, Sugimura H: Expression of high-mobility group-1 mRNA in human gastrointestinal adenocarcinoma and corresponding non-cancerous mucosa. Int J Cancer 1997, 74:1–6
27. Lee S, Baek M, Yang H, Bang YJ, Kim WH, Ha JH, Kim DK, Jeoung DI: Identification of genes differentially expressed between gastric cancers and normal gastric mucosa with cDNA microarrays. Cancer Lett 2002, 184:197–206
28. Ikenoue T, Ijichi H, Kato N, Kanai F, Masaki T, Rengifo W, Okamoto M, Matsumura M, Kawabe T, Shiratori Y, Omata M: Analysis of the β-catenin/T cell factor signaling pathway in 36 gastrointestinal and liver cancer cells. Jpn J Cancer Res 2002, 93:1213–1220
29. Hino S, Michiue T, Asashima M, Kikuchi A: Casein kinase Iε enhances the binding of Dvl-1 to Frat-1 and is essential for Wnt-3a-induced accumulation of β-catenin. J Biol Chem 2003, 278:14066–14073